

Chapter 5

Stable Resonators

5.1 General Aspects

In this part the basic properties of both stable and unstable optical resonators with spherical mirrors are explained. We neglect the presence of an active medium inside the resonator and assume that both resonator mirrors exhibit 100% reflectance at the wavelengths considered. Resonators that do not provide amplification of the light are called passive resonators. Although the active medium is required to generate laser emission, the concept of the passive resonator is applicable to the investigation of the physics of laser radiation. The inclusion of the gain only modifies the resonator properties. The influence of the amplification upon the radiation characteristics of resonators will be discussed in Part IV.

A stable optical resonator generally consists of two mirrors with radii of curvature ρ_1 and ρ_2 separated by an optical distance $L = nL_0$ (L_0 : geometrical mirror spacing, n : index of refraction inside the resonator). The range of L within which a resonator is stable is determined by the condition that a ray launched inside the resonator parallel to the optical axis remains inside the resonator after an infinite number of bounces. Equivalent to this definition is the lack of self-reproducing spherical waves inside the resonator (eigensolutions of the ABCD law, see Sec. 1.3).

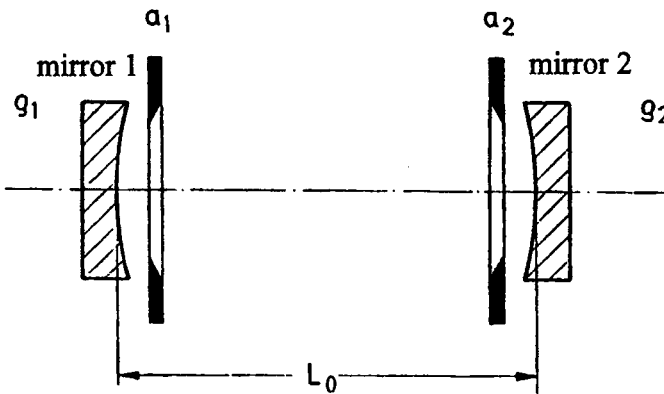


Fig. 5.1 The general optical resonator is determined by the g -parameters of the mirrors, the mirror spacing L_0 and the radii a_i of internal apertures.

By introducing the g -parameters of the resonator mirrors:

$$g_i = 1 - \frac{L}{\rho_i}, \quad i=1,2 \tag{5.1}$$

the condition for a stable resonator reads:

$$0 < g_1 g_2 < 1 \tag{5.2}$$

As discussed in Sec. 2.8.2, stable resonators exhibit a Gaussian beam as the fundamental eigenmode. Note that the radius of curvature is positive for a concave mirror and negative for a convex mirror. In Fig. 5.1 both radii of curvature are positive. It is convenient to visualize optical resonators in the g -diagram, also referred to as the stability diagram, in which a resonator is determined by a point in the g_1, g_2 plane (Fig. 5.2). The area of stable resonators is limited by the coordinate axes and the hyperbolas $g_2 = \pm 1/g_1$. The resonators on the stability limits, represent a unique class of resonators since the Gaussian beam is not an eigensolution of the electric field. The exception is the confocal resonator with $g_1 = g_2 = 0$ which is usually considered a stable resonator. However, since it exhibits some properties that are quite unique compared to common stable resonators, we will discuss the stable confocal resonator as well as resonators on the stability limits in a later section.

An optical resonator is generally defined by the g -parameters of the mirrors, the mirror spacing, and the dimensions of apertures that might be located inside the resonator. The goal of this chapter is to achieve a detailed understanding of how the mode structure and the diffraction losses are affected by these resonator parameters. We will first assume that there is no aperture inside the resonator and both mirrors have infinite lateral dimensions.

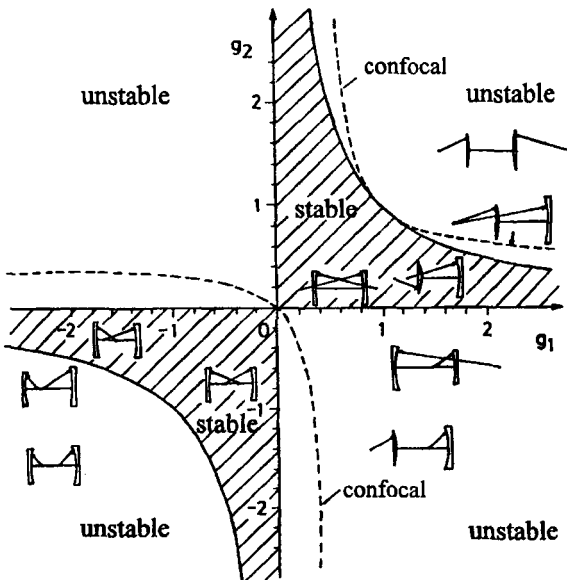


Fig. 5.2 The stability diagram of optical resonators with spherical mirrors. The hatched area indicates the region of stable resonators.

5.2 Unconfined Stable Resonators

We first want to know which field distributions on the resonator mirrors represent the steady-state solutions of the stable resonator. Such an eigensolution $E_i(x,y)$ on mirror i will reproduce itself after each round trip. The round trip in the resonator is described mathematically by the Kirchoff integral equation derived in Sec. 2.7.1 [3.7,3.10,3.16-3.20,3.24,3.25]:

$$\gamma E_i(x_2,y_2) = i \frac{\exp[-ikL]}{2Lg_j\lambda_0} \iint E_j(x_1,y_1) \exp\left[\frac{-i\pi}{2Lg_j\lambda_0} \left(G(x_1^2+y_1^2+x_2^2+y_2^2) - 2(x_1x_2+y_1y_2)\right)\right] dx_1 dy_1$$

with: $G = 2g_1g_2 - 1; \quad i,j=1,2; \quad i \neq j$ (5.3)
 L : optical resonator length $= nL_0$ (L_0 : geometrical length)
 λ_0 : vacuum wavelength, $k=2\pi/\lambda_0$: wave number

The solutions to this integral equation represent the eigenmodes of the optical resonator. In general an infinite number of eigenmodes exist. The field distributions of the eigenmodes do not change their shapes but they might experience a decrease in amplitude due to diffraction losses. This is taken into account by the complex eigenvalue γ . The loss factor,

$$V = |\gamma|^2, \tag{5.4}$$

represents the fraction of the initial power hitting the mirror after the round trip. The loss factor V is related to the loss ΔV via $\Delta V = 1 - V$. If both resonator mirrors are unconfined and perfectly reflecting, no power is lost during the round trip and the loss factor, therefore, is equal to 1.0. The condition $\gamma = 1.0$, referred to as the *resonance condition* of the optical resonator, yields the resonance frequencies.

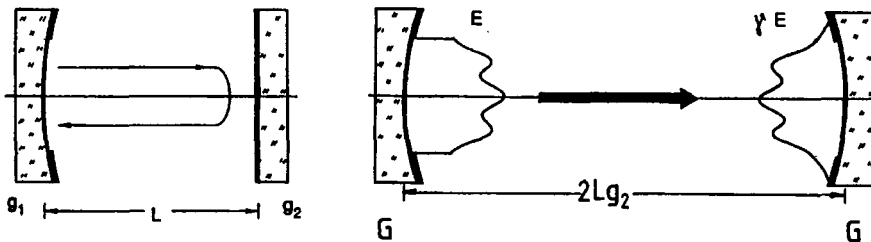


Fig. 5.3 A steady-state field distribution $E(x,y)$ must reproduce itself after each round trip. On the right side the round trip is presented as a transit in the equivalent resonator (see Sec. 5.3.2).

5.2.1 Transverse Mode Structures

Equation (5.3) can be solved analytically yielding an infinite number of eigensolutions. Which of these eigensolutions will actually be observed in the resonator depends on the geometry and the size of the mirrors. In reality, the mirrors will have a finite size with a shape that usually is round or rectangular. This boundary condition is taken into account by choosing those eigensolutions that exhibit circular or rectangular symmetry, respectively. The solutions to (5.1) for the two symmetries are described below (the index i denotes the mirror) [3.1,3.5,3.7]:

a) Circular Symmetry (Gauss-Laguerre Modes):

$$E_{p\ell}^{(i)}(r, \Phi) = E_0 \left[\frac{\sqrt{2}r}{w_i} \right]^\ell L_p^{(\ell)} \left(\frac{2r^2}{w_i^2} \right) \exp \left[\frac{-r^2}{w_i^2} \right] \begin{cases} \cos(\ell\Phi) \\ \sin(\ell\Phi) \end{cases} \quad (5.6)$$

$$\gamma = \exp \left[ik \left(2L - \frac{\lambda_0}{\pi} (2p + \ell + 1) \operatorname{acos} \sqrt{g_1 g_2} \right) \right] \quad (5.7)$$

with $L_p^{(\ell)} [t]$: Laguerre polynomial of order p, ℓ , p, ℓ integer
 r, Φ : radial and azimuthal coordinate
 k : wave number = $2\pi/\lambda_0$; λ_0 : wavelength in vacuum
 L : optical mirror spacing = nL_0

The Laguerre polynomials can be found in mathematical handbooks [3.13,3.14]. For low orders p, ℓ they read:

$$L_0^{(\ell)}(t) = 1$$

$$L_1^{(\ell)}(t) = \ell + 1 - t$$

$$L_2^{(\ell)}(t) = 0.5(\ell+1)(\ell+2) - (\ell+2)t + 0.5t^2$$

$$L_3^{(\ell)}(t) = (\ell+1)(\ell+2)(\ell+3)/6 - 0.5(\ell+2)(\ell+3)t + 0.5(\ell+3)t^2 - t^3/6$$

b) Rectangular Symmetry (Gauss-Hermite Modes):

$$E_{mn}^{(i)}(x, y) = E_0 \exp \left[\frac{-(x^2 + y^2)}{w_i^2} \right] H_m \left(\frac{\sqrt{2}x}{w_i} \right) H_n \left(\frac{\sqrt{2}y}{w_i} \right) \quad (5.8)$$

$$\gamma = \exp \left[ik \left(2L - \frac{\lambda_0}{\pi} (m+n+1) \operatorname{acos} \sqrt{g_1 g_2} \right) \right] \quad (5.9)$$

The Hermite polynomials H_m can also be looked up in mathematical handbooks. For low order numbers m, n they read:

$$\begin{aligned} H_0(t) &= 1 & H_1(t) &= 2t \\ H_2(t) &= 4t^2 - 2 & H_3(t) &= 8t^3 - 12t \\ H_4(t) &= 16t^4 - 48t^2 + 12 & H_5(t) &= 32t^5 - 160t^3 + 120t \end{aligned}$$

In both symmetries the loss factor V is equal to 1.0 since the mirrors are not limited by an aperture and, consequently, no power can leak out of the resonator. Figure 5.4 presents intensity distributions as a function of the order numbers p, ℓ and m, n , calculated with (5.6) and (5.8), respectively.

The steady-state electric field distribution is characterized by the indices plq and mnq , whose meaning becomes apparent by looking at Fig. 5.4. In rectangular symmetry the first two indices represent the number of nodal lines of the intensity distribution in the corresponding direction. In circular symmetry the intensity distributions exhibit p radial and ℓ azimuthal nodes at which the intensity is equal to zero. The index q was already discussed in Chapter 4; it represents the number of half wavelengths fitting into the mirror spacing.

A steady-state field distribution oscillating inside the resonator is called an eigenmode of the resonator. The eigenmodes are characterized by the transverse mode structure (transverse mode index p, ℓ or m, n) and the axial mode order q . The notations for the eigenmodes are

$$TEM_{p\ell q} \quad \text{and} \quad TEM_{mnq}$$

where the abbreviation TEM represents the fact that the electric and the magnetic field vectors are perpendicular to each other and to the wave vector k (Transverse Electro Magnetic). This is not entirely true since the diffraction generates small field components in the direction of the wave propagation (see Sec. 2.9). Only in the limit of large beam radii (large Fresnel numbers) is the field truly transverse. The notation TEM was adopted from the modes of waveguides which in fact are transversal. Although not physically correct, it is customary to refer to the modes of open resonators as TEM modes as well. In general, the axial mode index q is not used and the mode structure is specified by the order numbers p, ℓ and m, n (as we have seen, q can be very large).

The lateral extent of the eigenmodes on mirror i is determined by the beam radius w_i of the TEM_{00} mode. The beam radii w_1 and w_2 on the two mirrors depend on the mirror spacing and the g -parameters of the resonator:

$$w_i^2 = \frac{\lambda L}{\pi} \sqrt{\frac{g_j}{g_i(1 - g_1 g_2)}}; \quad i, j = 1, 2; \quad i \neq j \tag{5.10}$$

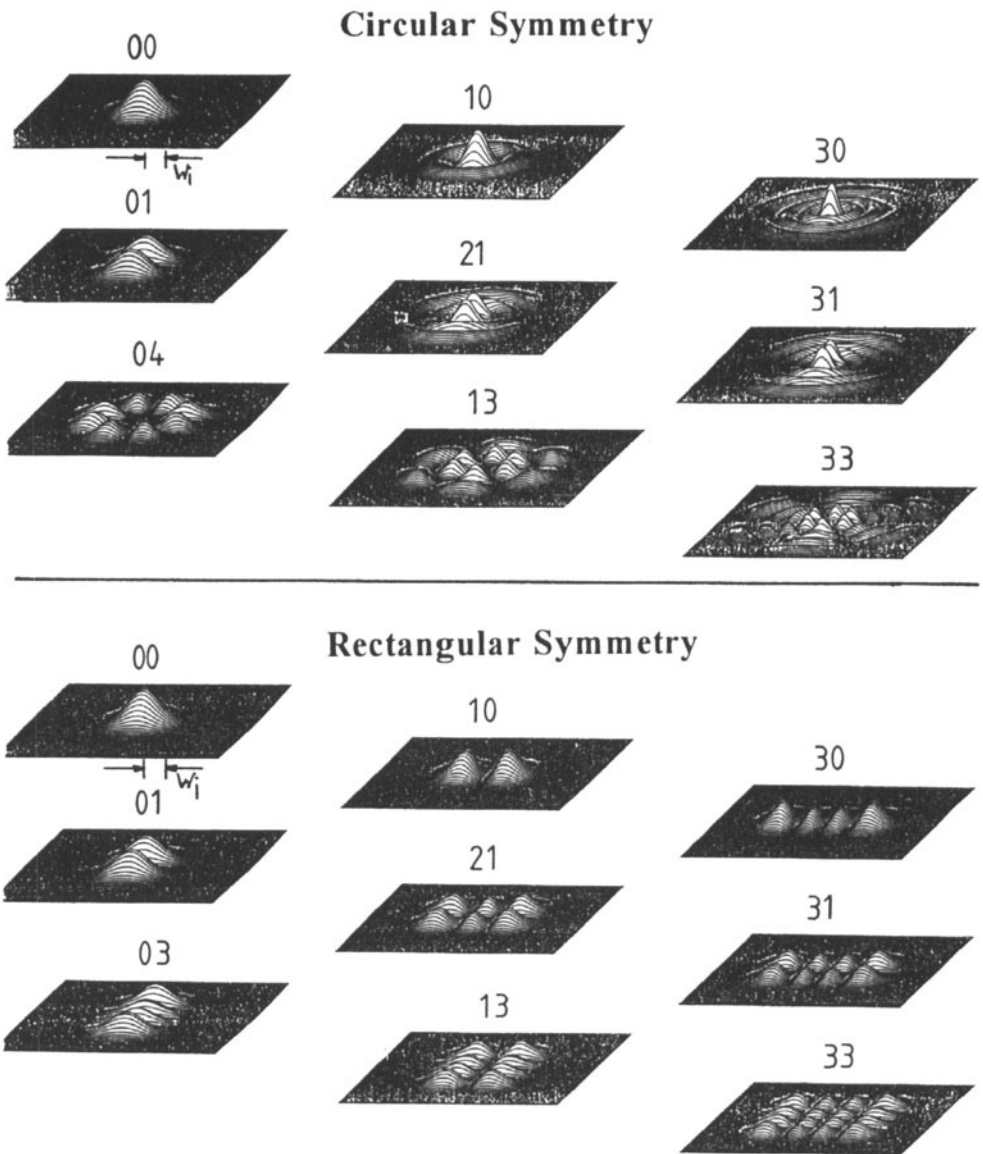


Fig. 5.4 Intensity distributions on the mirrors of stable resonators calculated with (5.6) and (5.8) for different mode orders $p\ell$ and mn . The radius w , is the same for all distributions [S.3].

As can be seen in Fig. 5.4, the size of the intensity distributions increases as the mode order is increased. In both symmetries the TEM_{00} mode has the same shape (Fig. 5.5); the intensity distribution is Gaussian. At a distance $r=w_1$ from the center of gravity, the intensity has decreased by a factor of $1/e^2$ and 86.5% of the beam power is contained within the corresponding circle. The lateral extent of the TEM_{00} mode is therefore defined by the beam radius w_1 , also referred to as the Gaussian beam radius. The TEM_{00} mode is the mode with the smallest size that can oscillate in a stable resonator. It is generally referred to as the *fundamental mode* or the Gaussian beam.

For transverse modes of higher order p or mn , the beam radii are defined via the second intensity moments introduced in Chapter 2.6 (see Eqs. (2.93) and (2.97)). This definition of the beam radii enables one to calculate the propagation of arbitrary field distributions through ABCD-type optics by applying the generalized ABCD law (2.111)(see Sec. 2.6).

The beam radii on mirror i read [3.31,3.32]:

Circular Symmetry: $w_{pi}^{(i)} = w_i \sqrt{2p + 1 + 1}$ (5.11)

Rectangular Symmetry: $w_{mn}^{(i)} = w_i \sqrt{2m + 1}$ *x-direction* (5.12)

$w_{mn}^{(i)} = w_i \sqrt{2n + 1}$ *y-direction* (5.13)

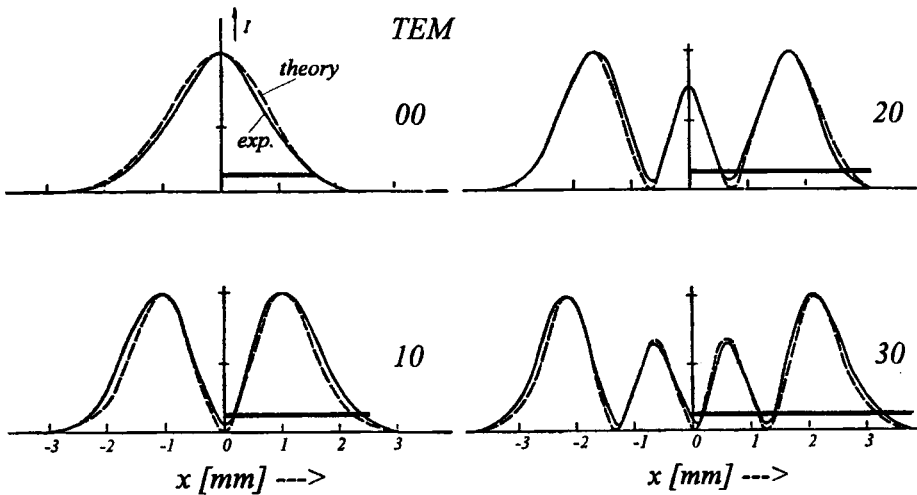


Fig. 5.5 Measured (solid line) and calculated (dashed line) one-dimensional intensity distributions of transverse modes TEM_{mn} in rectangular symmetry. The horizontal lines indicate the beam radii w_{m0} defined by the second intensity moments.

Note that, as far as the power content is concerned, the second intensity moments yield beam radii that are too large, especially for modes in rectangular symmetry. For higher order modes the power fraction contained within the radius $w_{pl}^{(i)}$ is greater than 86.5%. Table 5.1 shows the difference between the beam radii and the 86.5% power content radii for different mode orders p, ℓ and m, n . For some laser applications it may be more applicable to define the beam radii via the 86.5% energy content. However, since the beam propagation can be calculated for arbitrary field distributions with the ABCD law (2.111), the definition of the beam radius using the second intensity moments was standardized by ISO for the measurement of beam quality, beam diameter and beam divergence [1.86]. As far as the modes of stable resonators are concerned, the generalized ABCD law can also be applied to the power content radii (see Fig. 2.20) provided that the far field angle is defined the same way.

In order to get a better agreement with the power content radii, we modify the beam radii for rectangular symmetry modes by dividing by $\sqrt{2}$:

$$w_{mn}^{(i)} = w_i \sqrt{m+1/2} \quad x\text{-direction}$$

Table 5.1 Calculated ratio of 86.5% power content beam radii $r_{86.5\%}$ to the beam radii w_{pl} defined via the second intensity moment for transverse modes of stable resonators in circular and rectangular symmetry (Eqs. (5.11), (5.12)). For comparison: a homogeneous circular intensity profile with radius R yields a second moment radius of $w_{pl}=R$ and an 86.5% power content radius of $r_{86.5\%}=0.93R$ (ratio of 0.93). The radius ratio for a homogeneous intensity profile of width $2a$ is $(0.865a)/(2a/\sqrt{3})=0.749$.

p	ℓ	$r_{86.5\%}/w_{pl}$	p	ℓ	$r_{86.5\%}/w_{pl}$
0	0	1.000	0	7	0.853
1	0	0.960	0	10	0.813
4	0	0.960	0	100	0.746
7	0	0.960	0	∞	$1/\sqrt{2}$
∞	0	0.960	1	10	0.865
0	1	0.944	4	10	0.920
0	4	0.857	7	10	0.941

m	n	$r_{86.5\%}/w_{mn}$	m	n	$r_{86.5\%}/w_{mn}$
0	0	0.740	3	3	0.667
1	1	0.678	4	4	0.665
2	2	0.670	5	5	0.664

If we use the modified beam radii in rectangular symmetry, the ratio of the 86.5% power content radius to the modified beam radius is increased to about 0.94 for higher order modes and to 1.05 for the fundamental mode. However, we have to apply the same correction factor of $1/\sqrt{2}$ to the angles of divergence in order to preserve the validity of the generalized ABCD law (2.111). The modified beam radius gives the position of the outermost inflection point of the intensity distribution. To be consistent in our notation for the beam radii, we will use $w_{00}^{(i)}$ instead of w_i for the beam radius of the fundamental mode (Gaussian beam) on mirror i . Let us first look at some examples to get a feeling for the transverse mode size of stable resonators.

Examples:

a) HeNe laser, circular symmetry, $\lambda=632.8\text{nm}$, $L=1\text{m}$, $\rho_1=\rho_2=2\text{m}$.

$$w_{00}^{(1)} = w_{00}^{(2)} = 0.4823 \text{ mm}$$

$$w_{10}^{(1)} = w_{10}^{(2)} = 0.8354 \text{ mm}$$

$$w_{11}^{(1)} = w_{11}^{(2)} = 0.9646 \text{ mm}$$

b) HeNe laser, circular symmetry, $\lambda=632.8\text{nm}$, $L=1\text{m}$, $\rho_1=5\text{m}$, $\rho_2=\infty$ (flat).

$$w_{00}^{(1)} = 0.7092 \text{ mm} \quad w_{00}^{(2)} = 0.6437 \text{ mm}$$

$$w_{10}^{(1)} = 1.2284 \text{ mm} \quad w_{10}^{(2)} = 1.0992 \text{ mm}$$

$$w_{11}^{(1)} = 1.4184 \text{ mm} \quad w_{11}^{(2)} = 1.2692 \text{ mm}$$

c) CO₂ laser, circular symmetry, $\lambda=10,600 \text{ nm}$, $L=1\text{m}$, $\rho_1=5\text{m}$, $\rho_2=\infty$ (flat).

$$w_{00}^{(1)} = 2.9026 \text{ mm} \quad w_{00}^{(2)} = 2.5972 \text{ mm}$$

$$w_{10}^{(1)} = 5.0275 \text{ mm} \quad w_{10}^{(2)} = 4.4984 \text{ mm}$$

$$w_{11}^{(1)} = 5.8052 \text{ mm} \quad w_{11}^{(2)} = 5.1944 \text{ mm}$$

The cross sectional area of the Gaussian beam radius scales linearly with the wavelength and the resonator length. It is for this reason that CO₂ lasers with their large emission wavelength of 10.6 μm exhibit relatively large beam radii of the fundamental mode. On the other hand, diode lasers have very small Gaussian beam radii on the order of μm due to their short mirror spacing in the sub-mm range. Furthermore, at a fixed wavelength and a fixed resonator length, the Gaussian beam radius will decrease as the resonator design is chosen

closer to a stability limit in the g -diagram. This fact is visualized in Fig. 5.6 which presents curves of constant cross sectional area of the Gaussian beam at mirror 1. The beam radius at mirror 2 can be obtained from this graph by switching g_1 and g_2 .

The transverse modes that are actually observed in a laser resonator, are mainly determined by the size of the mirrors. The resonator mirrors are generally limited either by apertures or by the active medium itself. Only those transverse modes whose beam radii are smaller than the radii of the mirror apertures can be observed. This means that only modes up to a certain transverse order are allowed to oscillate. Modes with higher transverse orders exhibit losses that are too high to be compensated by the gain medium. If the gain of the medium is increased, more transverse modes will, however, reach the laser threshold. As a rule of thumb, a higher order transverse mode will oscillate if the radius of the aperture a is greater than 0.9-1.0 times the beam radius. Fundamental mode operation requires an aperture radius a of 0.9-1.3 times the Gaussian beam radius. Upper values and lower values correspond to low gain and to high gain active media, respectively.

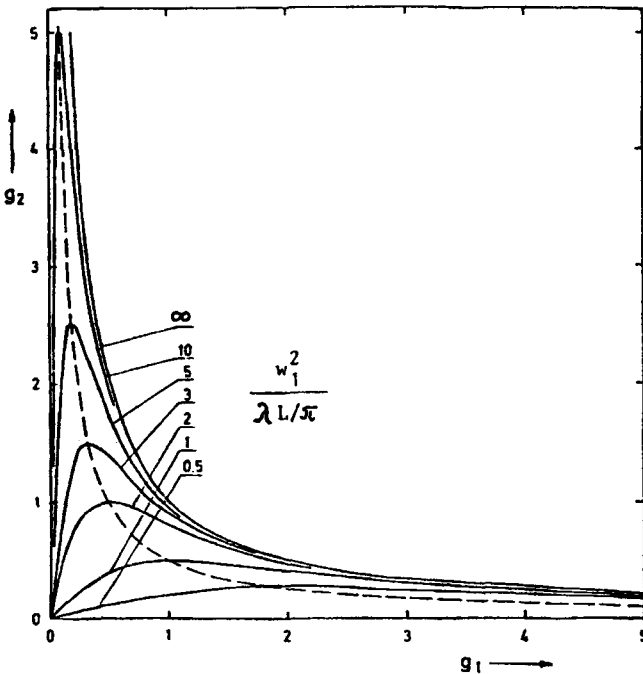


Fig. 5.6 Curves of constant cross sectional area of the Gaussian beam at mirror 1 in the stability diagram. The cross sectional area is normalized to $\lambda L/\pi$. The beam radius at mirror 2 can be obtained by switching g_1 and g_2 .

Example:

HeNe laser, circular symmetry, $\lambda=632.8\text{nm}$, $L=0.3\text{m}$, $\rho_1=5\text{m}$, $\rho_2=3\text{m}$. The mirrors are close to the endfaces of the discharge tube with inner diameter of $2a=3\text{mm}$.

According to (5.10), the Gaussian beam radii on the mirrors are $w_{00}^{(1)}=0.388\text{mm}$ and $w_{00}^{(2)}=0.397\text{mm}$. Only those transverse modes are observed for which the beam radii at both mirrors are smaller than the tube radius:

$$a \geq 1.0 w_{00}^{(j)} \sqrt{2p + \ell + 1}$$

This is equivalent to the condition $2p + \ell + 1 \leq 14$. The transverse modes with the highest radial and highest azimuthal order oscillating in the HeNe laser are TEM_{60} and TEM_{012} , respectively.

Lasers can be forced to oscillate only in the fundamental mode by inserting apertures into the resonator with a diameter close to the diameter of the Gaussian beam at the aperture plane. If the apertures are considerably larger than the Gaussian beam, all higher transverse modes fitting into the aperture will oscillate. It is for this reason that in multimode lasers one does generally not observe the characteristic intensity distributions of Fig. 5.4. Since all of these modes exhibit virtually no loss, they are oscillating simultaneously resulting in a more or less homogenous beam profile. The more modes that participate in this process the more homogenous the laser beam becomes. This multimode behavior is supported by the fact that different modes exhibit their intensity maxima in different areas of the active medium. The gain at the nodal lines of the intensity distribution is not depleted and can then be used by a different mode that has its intensity peaks in these vacant areas. Figure 5.7 presents a photograph of the intensity distribution at the output coupling mirror of a Nd:YAG rod laser. The large rod diameter of 10mm enables all transverse modes with $2p + \ell + 1 < 60$ to oscillate. The high number of modes results in a good homogeneity of the beam.

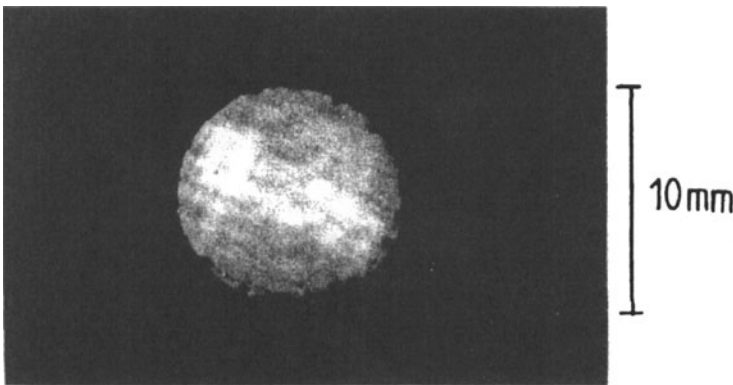


Fig. 5.7 Photograph of the beam profile of a Nd:YAG rod laser ($\lambda=1.064\mu\text{m}$) with a stable resonator in multimode operation (maximum of $2p + \ell + 1$ is about 60).

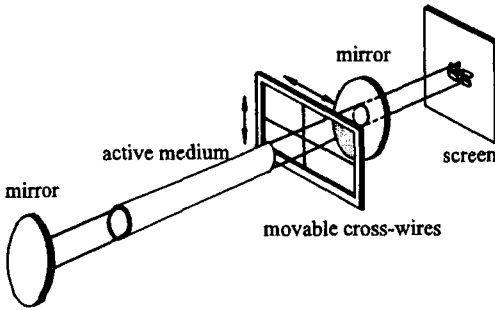


Fig. 5.8 Set-up to observe the transverse intensity distributions of individual transverse modes in a multimode laser.

It is possible to observe the intensity structure of individual transverse modes by generating losses for all other modes. One technique to accomplish this is to insert cross-wires into the resonator as depicted in Fig. 5.8. The mode having nodal lines along the wires is preferred since it experiences lower losses than all other modes. By moving the cross wires, different transverse modes can be selected. Due to the symmetry of the obstruction, only modes with rectangular symmetry are observed. The intensity distributions of the modes of a HeNe laser shown in the photographs of Fig. 5.9 were generated this way.

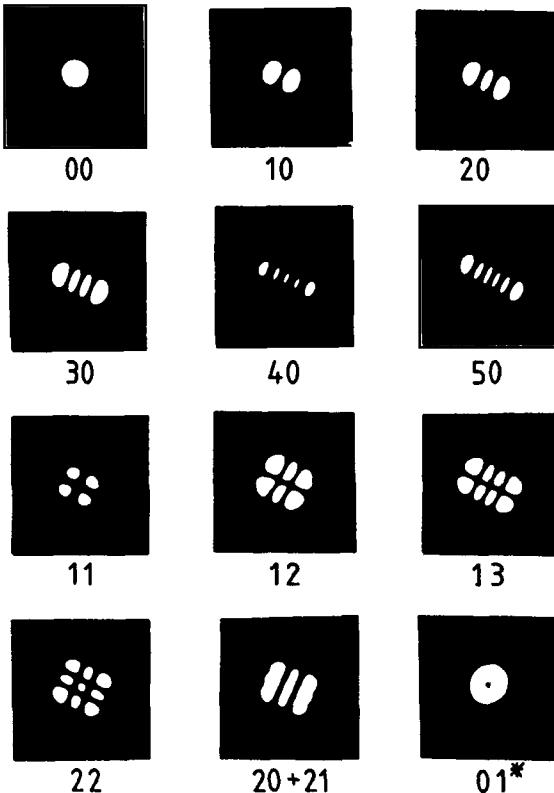


Fig. 5.9 Photographs of intensity distributions of different transverse modes at the output coupling mirror of a HeNe laser with a stable resonator. The cross-wires select modes with rectangular symmetry. The lower right photograph shows the lowest order donut mode (without cross-wires).

Hybrid Modes

In circularly symmetric laser resonators one can quite often observe intensity distributions of modes that exhibit an annular intensity profile with almost zero intensity in the center. These beam profiles are generated by a superposition of two circularly symmetric transverse modes of the same order $p\ell$ which are both linearly polarized and oscillate rotated by an angle of 90° with respect to each other (Fig. 5.10). There are four different ways to combine two linearly polarized modes resulting in different polarization states of the sum mode. The superposition always yields the same annular intensity profile with $p+1$ rings with maximum intensity and a characteristic hole in the center. It is quite obvious why these modes are called donut modes. Sometimes they are also referred to as hybrid modes. Hybrid modes are marked by an asterisk next to the mode order numbers. Due to the different polarizations, the two transverse modes do not interfere and the intensity distribution of the sum is given by the sum of the individual mode intensity profiles. Application of (5.6) yields for the radial intensity distribution of hybrid modes at mirror i :

$$I_{p\ell}^*(t) = I_0 t^\ell \exp[-t] [L_{p\ell}(t)]^2, \tag{5.14}$$

with $t = 2 \left[r/w_{00}^{(i)} \right]^2$.

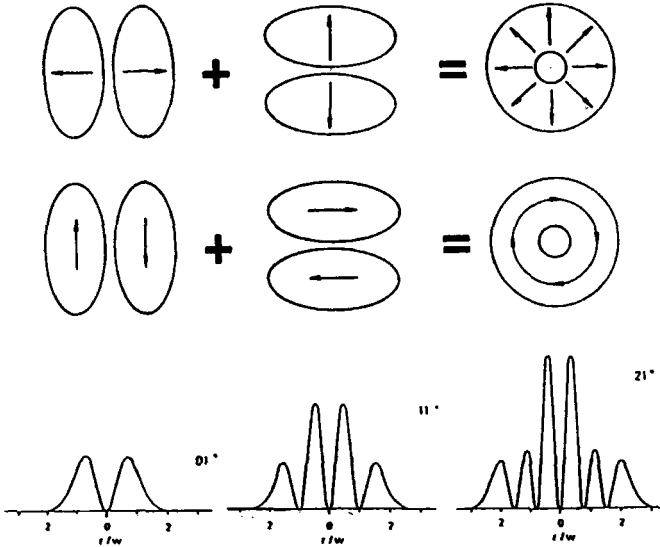


Fig. 5.10 Hybrid modes are generated by the superposition of two linearly polarized circularly symmetric transverse modes of the same order $p\ell$ which oscillate rotated by 90° with respect to each other. The graph shows two of the four possible ways to superimpose the mode structures. The lower graphs present the radial intensity distributions of the three lowest order hybrid modes TEM_{01}^* , TEM_{11}^* , and TEM_{21}^* .

Hybrid modes are quite often observed if an aperture inside the resonator is continuously varied. As an example, Fig. 5.11 presents the development of the beam profile of an Nd:YAG laser as the diameter of an aperture inside the stable resonator is increased. Although these intensity distributions represent the superposition of more than two transverse modes, they often exhibit the center hole characteristic of hybrid modes.

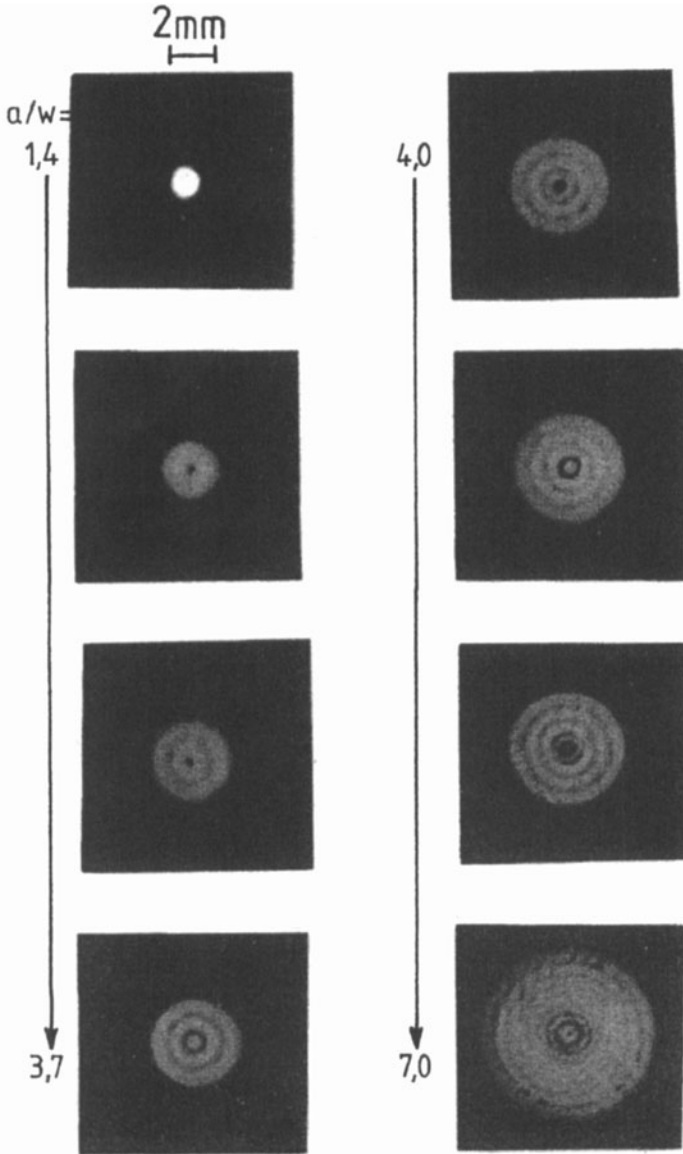


Fig. 5.11 Photographs of intensity distributions at the output coupling mirror of an Nd:YAG rod laser. The radius a of an aperture located inside the stable resonator is increased; w denotes the Gaussian beam radius at the aperture ($g_1=1$, $g_2=0.5$, $L=0.5m$, $\lambda=1.064\mu m$).

5.2.2 Resonance Frequencies

The development of steady-state field distributions in any optical resonator requires that both the amplitude and the phase of the electric field $E(x, y)$ are reproduced after each round trip. According to (5.3) this requirement is met if the eigenvalue γ is equal to 1.0, which is referred to as the *resonance condition*. Together with (5.7) and (5.9), the resonance condition yields the resonance frequencies ν of the eigenmodes [3.7]:

$$\text{Circular Symmetry:} \quad \nu_{plq} = \frac{c_0}{2L} \left[q + \frac{2p+\ell+1}{\pi} \operatorname{acos}\sqrt{g_1 g_2} \right] \quad (5.15)$$

$$\text{Rectangular Symmetry:} \quad \nu_{mnq} = \frac{c_0}{2L} \left[q + \frac{m+n+1}{\pi} \operatorname{acos}\sqrt{g_1 g_2} \right] \quad (5.16)$$

with c_0 : speed of light in vacuum
 L : optical mirror spacing = nL_0 (L_0 : geometrical spacing,
 n : index of refraction inside the resonator)

The resonance frequencies thus depend on both the axial and the transverse mode order. In contrast to the plane-parallel FPI ($g_1=g_2=1$, Sec. 4.1) whose resonance frequencies are only determined by the axial mode index, each axial mode of stable resonators is subdivided into a sequence of frequencies corresponding to different transverse modes. This separation is controlled by the g -parameters of the resonator mirrors (Fig. 5.12). As the origin of the g -diagram is approached, the frequency gap between different transverse modes having the same axial mode order becomes wider. In the limit of the stable confocal resonator ($g_1=g_2=0$), the frequency gap equals $c_0/(4L)$ which is half the axial mode distance. The confocal resonator exhibits frequency degeneracy which means that all modes meeting the conditions $2q + 2p + \ell + 1 = k$ and $2q + m + n + 1 = k$, with k : integer, oscillate at the same resonance frequency $kc_0/(4L)$.

The difference in resonance frequencies plays an important role in the temporal stability of the laser emission. If several transverse modes oscillate, the emission is modulated with the difference frequencies of the modes, called the beat frequency (Fig. 5.13). Chaotic laser emission can occur if more than two transverse modes oscillate simultaneously. Lasers featuring a stabilized temporal output operate at one single transverse mode (usually the fundamental mode) and preferably at one single axial mode. Single transverse mode operation is usually achieved by aperture-limiting the Gaussian beam inside the resonator. Single axial mode operation can be attained with one or a combination of the following techniques (depending on the type of laser): a) reduction of the gain bandwidth with intracavity etalons, gratings, or Lyot filters, b) increase of the axial mode spacing by using longer resonators or coupled resonators, c) prevention of standing waves inside the active medium (unidirectional ring resonator, twisted mode resonator) (see also Chapter 21).

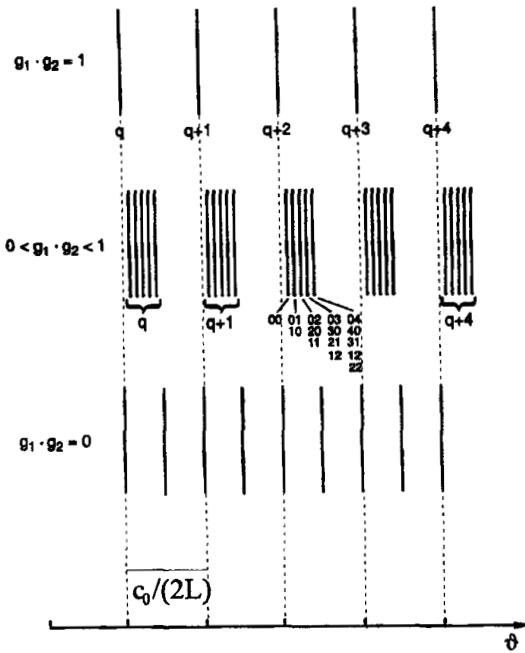


Fig. 5.12 Resonance frequencies of the modes of stable resonators with rectangular symmetry for different g -parameter products. The indices mn of some transverse modes are shown for the axial mode of order $q+2$.

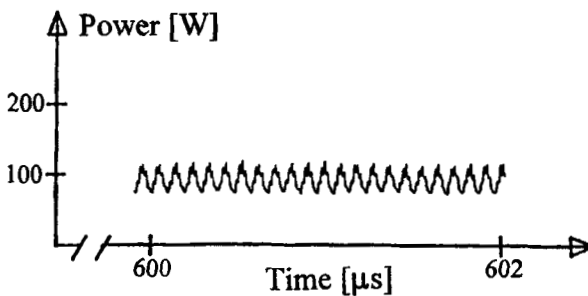
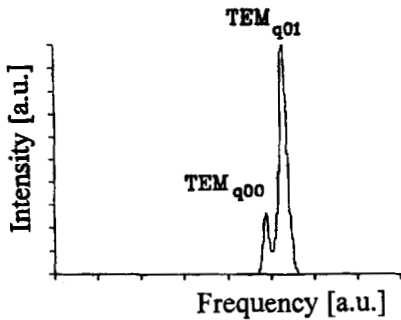


Fig. 5.13 Measured frequency spectrum of a pulsed single axial mode Nd:YAG ring laser ($L=1m$, $g_1 = g_2 = 0.5$) operating at two transverse modes and the temporal emission [S.4]. The beat frequency is 45MHz. The additional modulation at 12MHz is caused by the nonlinear interaction between the modes in the active medium (sloshing of power between the modes).

5.2.3 The TEM₀₀ Mode

So far we have only discussed the intensity distributions of the modes at the resonator mirrors and how the mode structure depends on the resonator length and the g-parameters of the mirrors. The Gaussian beam radius $w_{00}^{(i)}$ at mirror i determines the lateral dimension of the mode. For stable resonators, the intensity distributions at any plane inside or outside the resonator exhibit the same shape as the distributions on the mirrors; only the beam radius changes with the propagation.

For the fundamental mode, or Gaussian beam, the beam radius as a function of the distance can be calculated by using the ABCD law (2.51). If z denotes the distance along the optical axis from the position of the beam waist with radius w_0 , the Gaussian beam radius $w_{00}(z)$ inside the resonator reads (Fig. 5.14):

$$w_{00}(z) = w_0 \sqrt{1 + \left(\frac{z}{z_0}\right)^2} \tag{5.17}$$

with:

$$\text{waist radius } w_0^2 = \frac{\lambda L}{\pi} \frac{\sqrt{g_1 g_2 (1 - g_1 g_2)}}{|g_1 + g_2 - 2g_1 g_2|} \tag{5.18}$$

$$\text{Rayleigh range } z_0 = \frac{\pi w_0^2}{\lambda} \tag{5.19}$$

$$\text{waist position } L_{01} = L \frac{(1 - g_1)g_2}{|g_1 + g_2 - 2g_1 g_2|} \tag{5.20}$$

The waist position L_{01} is the distance of the minimum beam radius (beam waist) from mirror 1. If L_{01} is positive the waist is located to the right of mirror 1 (as shown in Fig. 5.14), for a negative L_{01} the waist is found to the left of mirror 1 (see Fig. 5.15).

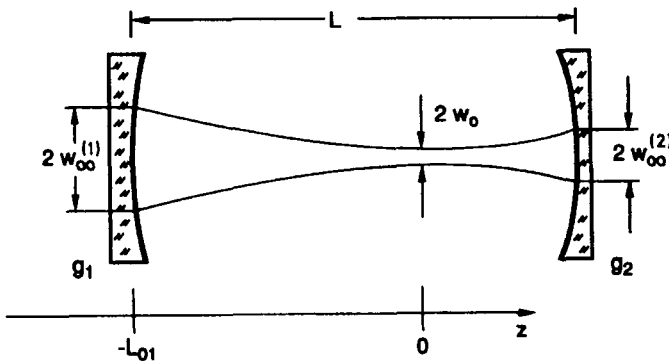


Fig. 5.14 Propagation of a Gaussian beam in a stable resonator.

At the distance of one Rayleigh range z_0 from the position of the beam waist the beam radius has increased by a factor of $\sqrt{2}$, which means that the cross sectional area of the beam has doubled. The physical meaning of the Rayleigh range will be discussed in Sec. 5.2.5. If we insert the values $z=L_{01}$ and $z=L-L_{01}$ into (5.17) we obtain expression (5.10) for the Gaussian beam radius on mirror 1 and mirror 2, respectively.

Example: Stable Resonator with $L=1.5\text{m}$, $\rho_1=-1\text{m}$, $\rho_2=2\text{m}$, $\lambda=632.8\text{nm}$ (Fig. 5.15)

The g -parameters of this resonator are $g_1=2.5$ and $g_2=0.25$. With (5.17)-(5.20) we obtain: $w_0 = 0.3123\text{mm}$, $z_0=485\text{mm}$, $L_{01}=-375\text{mm}$, $w_{00}^{(1)}=0.395\text{mm}$, $w_{00}^{(2)}=1.249\text{mm}$

The beam waist is located at a distance of 375mm to the left of mirror 1. It is for this reason that the beam radius on mirror 1 is much smaller than the beam radius on mirror 2, since the latter mirror is farther away from the beam waist.

The Gaussian beam is fully determined by the beam radius, the Rayleigh range, and the location of the beam waist. The divergence angle (half cone angle) θ_0 is obtained from these quantities by using the relation:

$$\theta_0 = \frac{\lambda}{\pi w_0} = \frac{w_0}{z_0} \tag{5.21}$$

The beam parameter product $w_0\theta_0$ is a constant of the Gaussian beam as long as the beam propagates through ABCD-type optical systems.

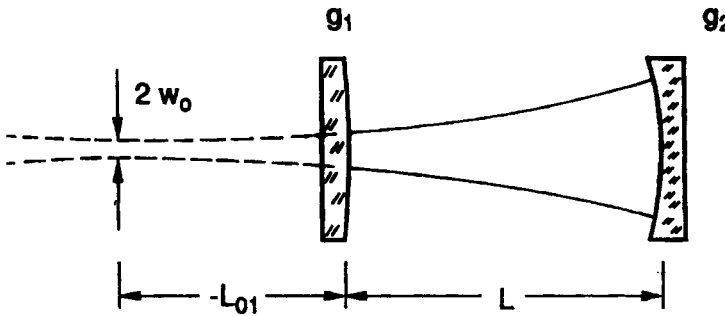


Fig. 5.15 A stable resonator with the beam waist being outside the resonator. According to (5.20), the distance L_{01} is negative.

The radius of curvature $R^{(i)}$ of the Gaussian beam at mirror i is always equal to the radius of curvature ρ_i of the mirror. The general expression for the radius of curvature R as a function of the propagation distance z reads:

$$R(z) = z_0 \left[\frac{z}{z_0} + \frac{z_0}{z} \right] \tag{5.22}$$

If we set $z=L_{0i}$ and $z=L-L_{0i}$ we can easily verify that the mirror surfaces indeed represent surfaces of constant phase of the Gaussian beam.

The general expression for the electric field of a Gaussian beam as a function of the distance z from the waist is given by:

$$E(x,y,z) = \frac{E_0}{\sqrt{1 + (z/z_0)^2}} \exp \left[\frac{-(x^2+y^2)}{w_{00}^2(z)} - \frac{ik(x^2+y^2)}{2R(z)} \right] \exp \left[-i \operatorname{atan} \left(\frac{z}{z_0} \right) \right] \tag{5.23}$$

The last term is referred to as the Gouy phase shift. This additional phase is the reason why the resonance frequency (5.15/5.16) has an additional term that depends on the g -parameters of the resonator. By introducing the q -parameter of the Gaussian beam:

$$\frac{1}{q(z)} = \frac{1}{R(z)} - \frac{i\lambda}{\pi w_{00}^2(z)} \tag{5.24}$$

the field distribution can be written as (see Eqs. 2.50/2.59):

$$E(x,y,z) = \frac{E_0}{\sqrt{1 + (z/z_0)^2}} \exp \left[-\frac{ik(x^2+y^2)}{2q(z)} \right] \exp \left[-i \operatorname{atan} \left(\frac{z}{z_0} \right) \right] \tag{5.25}$$

Propagation of the Gaussian beam through ABCD-type optics can be accomplished by using the ABCD-law (2.51) for the q -parameter. For the propagation of the Gaussian beam outside the resonator the imaging properties of the resonator mirrors have to be taken into account. In general, the mirror substrates have a planar rear surface and, therefore, act as lenses transforming the Gaussian beam into a new Gaussian beam (Fig. 5.16). The new divergence angle behind mirror i with refractive index n is given by:

$$\theta_{0i}^{*2} = \theta_0^2 \frac{g_i(1+g_1g_2(n^2-1)) + n^2(g_j-2g_1g_2)}{|g_1+g_2-2g_1g_2|} \tag{5.26}$$

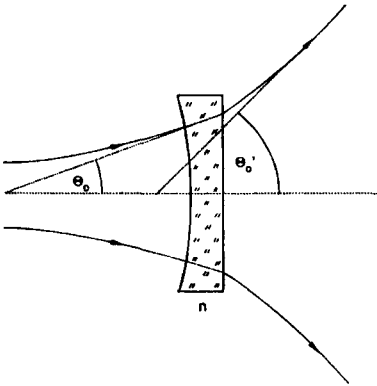


Fig. 5.16 Propagation through a mirror substrate changes the angle of divergence θ_0 of the Gaussian beam.

The two divergence angles are different for nonsymmetric resonators ($g_1 \neq g_2$) and usually greater than the intracavity divergence angle θ_0 . The new beam waist radius of the Gaussian beam behind mirror i can be determined with $w_{0i} = \lambda / (\pi \theta_{0i})$.

Resonator Schemes, Beam Radii, and Angles of Divergence of the TEM₀₀ Mode

The beam radii and the angles of divergence of common stable resonators are presented in Table 5.2 and in Fig. 5.17. The resonators on the stability limits have been included in this table to show that the beam waist radius goes to zero or infinity and, accordingly, the angle of divergence assumes values of $\pi/2$ or 0 if the stability limit is approached. This behavior is caused by the fact that a Gaussian beam is not an eigensolution of these resonators. The only exception is the confocal resonator located at the origin of the g -diagram.

Table 5.2 Stable resonators and the properties of their Gaussian beam.

Resonator	$(w_{00}^{(1)})^2$	$(w_{00}^{(2)})^2$	w_0^2	θ_0^2
symmetric ($g_1 = g_2 = g$)	$\frac{\lambda L}{\pi \sqrt{1-g^2}}$	$\frac{\lambda L}{\pi \sqrt{1-g^2}}$	$\frac{\lambda L \sqrt{1+g}}{2\pi \sqrt{1-g}}$	$\frac{2\lambda \sqrt{1-g}}{\pi L \sqrt{1+g}}$
plane-plane ($\rho_1 = \rho_2 = \infty, g_1 = g_2 = 1$)	∞	∞	∞	0
semi-confocal ($g_1 = 1, g_2 = 0.5$)	$\frac{\lambda L}{\pi}$	$\frac{2\lambda L}{\pi}$	$\frac{\lambda L}{\pi}$	$\frac{\lambda}{\pi L}$
symmetric confocal ($g_1 = g_2 = 0$)	$\frac{\lambda L}{\pi}$	$\frac{\lambda L}{\pi}$	$\frac{\lambda L}{2\pi}$	$\frac{2\lambda}{\pi L}$
general concentric ($\rho_1 + \rho_2 = L, g_1 g_2 = 1$)	∞	∞	0	$\pi^2/4$

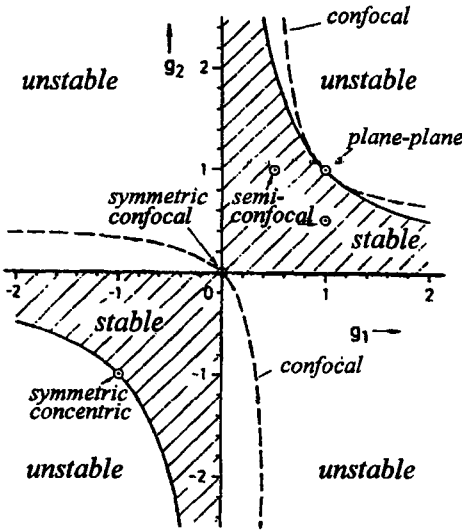


Fig. 5.17 The g-diagram of optical resonators and the location of common resonators.

Figure 5.18 presents the dependence of the angle of divergence on the resonator parameters. By combining (5.18) and (5.21), the angle of divergence θ_0 for a general stable resonator is given by:

$$\theta_0^2 = \frac{\lambda}{\pi L} \frac{|g_1 + g_2 - 2g_1g_2|}{\sqrt{g_1g_2(1 - g_1g_2)}} \tag{5.27}$$

The normalized angle $\theta_0\sqrt{L/\lambda}$ depends only on the g-parameters of the resonator. For a constant resonator length L , the angle of divergence becomes very small if the resonator is chosen close to the hyperbola in the first quadrant. The corresponding beam waist radius w_0 is, of course, very large for these resonators since the beam parameter product $w_0\theta_0$ is a constant. The largest angles of divergence are found for negative g-parameters at the stability limit $g_2=1/g_1$, where the concentric resonators are located. Since the large angles of divergence are generated by extremely small intracavity beam waists, these resonators have a small mode volume and have therefore found only limited application in laser systems.

Examples:

- | | | |
|---------------------------------------------------------------------------------------|------------------------|-----------------------------|
| 1) $L=1\text{m}, \lambda=1064\text{nm}$, semi-confocal: | $w_0=0.582\text{mm}$, | $\theta_0=0.582\text{mrad}$ |
| 2) $L=1\text{m}, \lambda=1064\text{nm}$, confocal: | $w_0=0.412\text{mm}$, | $\theta_0=0.823\text{mrad}$ |
| 3) $L=1\text{m}, \lambda=1064\text{nm}$, $\rho_1=-1.5\text{m}, \rho_2=1.5\text{m}$: | $w_0=0.435\text{mm}$, | $\theta_0=0.778\text{mrad}$ |
| 4) $L=1\text{m}, \lambda=1064\text{nm}$, $\rho_1=\infty\text{m}, \rho_2=5\text{m}$: | $w_0=0.823\text{mm}$, | $\theta_0=0.412\text{mrad}$ |
| 5) $L=1\text{m}, \lambda=1064\text{nm}$, $\rho_1=\rho_2=0.55\text{m}$: | $w_0=0.232\text{mm}$, | $\theta_0=1.463\text{mrad}$ |

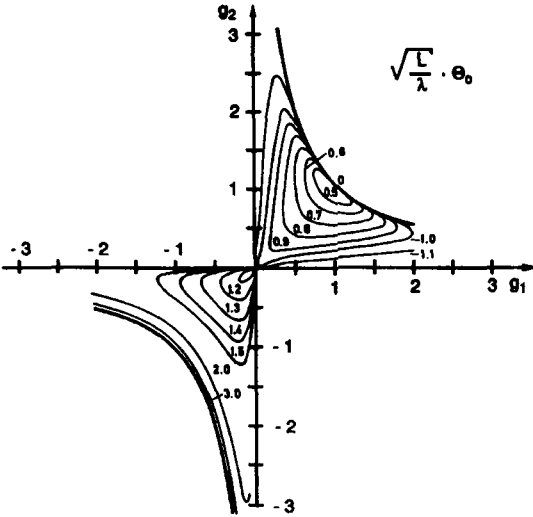


Fig. 5.18 Curves of constant angle of divergence θ_0 of the Gaussian beam in the g -diagram. The parameter is the normalized angle of divergence $\theta_0 \sqrt{L/\lambda}$ which is 1.0 for the confocal resonator.

Mode Volume of the TEM₀₀ Mode

The output power of a laser resonator, among other parameters, is determined by the volume of the active medium that is filled by the mode. Only in this area can the stored energy be extracted by the mode via induced emission. Let us calculate the volume of the Gaussian beam between the resonator mirrors assuming that the mode volume is determined by the Gaussian beam radius $w(z)$. As far as the output power is concerned, we consider an active medium that fills the whole resonator. Integration of the square of the beam waist $w(z)$ given by (5.17)-(5.19) from $z=-L_{o1}$ to $z=L-L_{o1}$ yields the mode volume of the Gaussian beam:

$$V_{00} = \pi\lambda L^2 \left[\frac{\sqrt{g_1 g_2 (1 - g_1 g_2)}}{|g_1 + g_2 - 2g_1 g_2|} \right] \left[1 + \frac{(g_2 - g_1)^2 + (1 - g_1)(1 - g_2)g_1 g_2}{3g_1 g_2 (1 - g_1 g_2)} \right] \quad (5.28)$$

The normalized mode volume $V_{00}/(\pi\lambda L^2)$ as a function of the g -parameters is shown in Fig. 5.19. It is apparent from this graph that the highest volume of the fundamental mode is achieved for resonators close to the stability limit at positive g -parameters and one g -parameter being much lower than 1. These resonators are formed by a concave and a convex mirror (see Fig. 5.15) and, therefore, are referred to as concave-convex resonators. A concave-convex resonator is the preferred means to achieve high output power in fundamental mode operation, even though they are more sensitive to mirror tilt than other resonators. Figure 5.20 presents measured output energies of a pulsed Nd:YAG laser in fundamental mode operation for different resonator configurations.

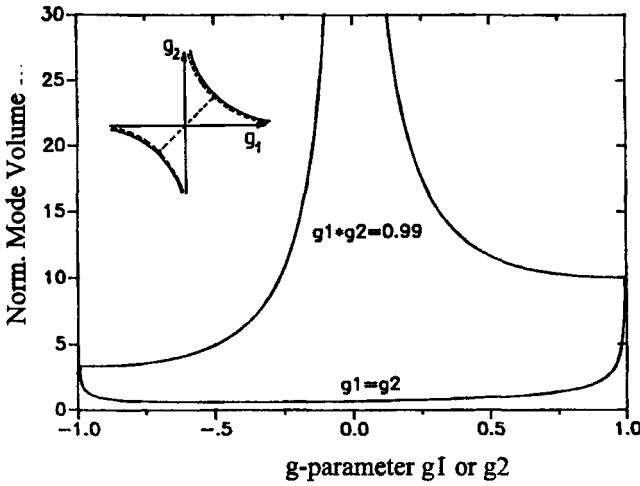


Fig. 5.19 Normalized mode volume $V_{00}/(\pi\lambda L^2)$ of the fundamental mode of stable resonators as a function of one of the g-parameters. The corresponding resonators are indicated in the g-diagram by dotted lines.

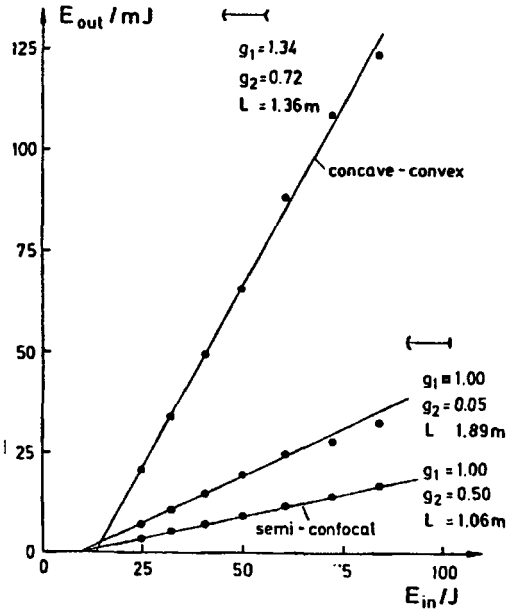


Fig. 5.20 Measured output energy of a pulsed $1.064\mu\text{m}$ Nd:YAG rod laser (rod diameter: 6.35mm , rod length: 76mm) in fundamental mode operation for different resonator configurations as a function of the electric energy supplied to the flashlamp.

5.2.4 Higher Order Modes

The treatment of the propagation of higher order modes in the resonators becomes quite simple given the preceding detailed discussion of the propagation of Gaussian beams. In both circular and rectangular symmetries the propagation of the fundamental mode and of the higher order modes is similar (Fig. 5.21). If w_0 and θ_0 denote the waist radius and the angle of divergence (half angle) of the fundamental mode, the beam radius as a function of the propagation distance from the waist position reads as follows:

a) in circular symmetry:

$$\text{beam radius at location } z: \quad w_{pl}(z) = w_0 \sqrt{2p+l+1} \sqrt{1 + \left(\frac{z}{z_0}\right)^2} \quad (5.29)$$

$$\text{waist radius:} \quad w_{pl} = w_0 \sqrt{2p+l+1} \quad (5.30)$$

$$\text{angle of divergence:} \quad \theta_{pl} = \theta_0 \sqrt{2p+l+1} \quad (5.31)$$

b) in rectangular symmetry:

$$\text{beam radius at location } z: \quad w_m(z) = w_0 \sqrt{2m+1} \sqrt{1 + \left(\frac{z}{z_0}\right)^2} \quad (5.32)$$

$$\text{waist radius:} \quad w_m = w_0 \sqrt{2m+1} \quad (5.33)$$

$$\text{angle of divergence:} \quad \theta_m = \theta_0 \sqrt{2m+1} \quad (5.34)$$

The Rayleigh range is the same as for the Gaussian beam:

$$z_0 = \frac{w_m}{\theta_m} = \frac{w_0}{\theta_0} = \frac{\pi w_0^2}{\lambda} \quad (5.35)$$

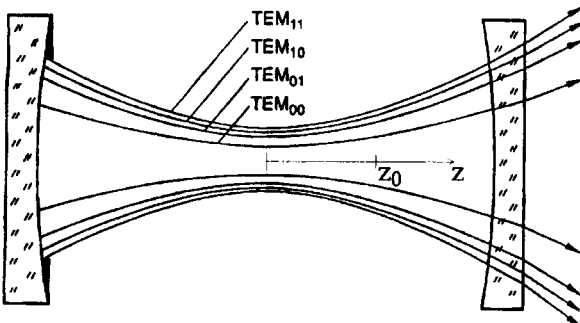


Fig. 5.21 Beam propagation of higher order modes. All modes have the same Rayleigh range. At any plane the beam radii are $\sqrt{2p+l+1}$ larger than the Gaussian beam radius.

The beam parameter product $w\theta$ is a constant of the beam with:

$$w_{pl}\theta_{pl} = (2p+l+1)\frac{\lambda}{\pi} = M^2\frac{\lambda}{\pi} \tag{5.36}$$

$$w_m\theta_m = (2m+1)\frac{\lambda}{\pi} = M^2\frac{\lambda}{\pi} \tag{5.37}$$

The term M^2 is referred to as the propagation factor of the mode. In a laser resonator, the maximum propagation factor corresponding to the highest order transverse mode determines the beam quality of the laser beam. Let us assume that N apertures with radii a_i are located inside the resonator at positions $z_1 \dots z_N$ and $w_{00}(z_i)$ are the beam radii of the Gaussian beam at the apertures. The maximum propagation factor, to a good approximation, is given by:

$$M^2_{\max} = \text{int} \min \left(\left[\frac{a_1}{w_{00}(z_1)} \right]^2, \left[\frac{a_2}{w_{00}(z_2)} \right]^2, \dots, \left[\frac{a_N}{w_{00}(z_N)} \right]^2 \right) \tag{5.38}$$

where min is the minimum term in the group and int rounds to the next integer value.

The electric field distribution of individual transverse modes as a function of the propagation distance z reads:

a) in circular symmetry: (5.39)

$$E(r, \Phi, z) = \frac{E_0}{\sqrt{1+(z/z_0)^2}} \exp \left[\frac{-r^2}{w_{00}^2(z)} - \frac{ikr^2}{2R(z)} \right] \left[\frac{\sqrt{2}r}{w_{00}(z)} \right]^\ell L_{pl} \left[\frac{2r^2}{w_{00}^2(z)^2} \right] \begin{cases} \cos(\ell\Phi) \\ \sin(\ell\Phi) \end{cases} \exp \left[-i(2p+l+1) \text{atan} \left(\frac{z}{z_0} \right) \right]$$

b) in rectangular symmetry: (5.40)

$$E(x, y, z) = \frac{E_0}{\sqrt{1+(z/z_0)^2}} \exp \left[\frac{-(x^2+y^2)}{w_{00}^2(z)} - \frac{ik(x^2+y^2)}{2R(z)} \right] H_m \left[\frac{\sqrt{2}x}{w_{00}(z)} \right] H_n \left[\frac{\sqrt{2}y}{w_{00}(z)} \right] \exp \left[-i(m+n+1) \text{atan} \left(\frac{z}{z_0} \right) \right]$$

The beam radius $w_{00}(z)$ and the radius of curvature $R(z)$ are those of the Gaussian beam (see (5.17) and (5.22)). The Gouy phase shift (far right term) generates the frequency difference between modes of different transverse order. By introducing the q-parameter:

$$\frac{1}{q(z)} = \frac{1}{R(z)} - \frac{i\lambda M^2}{\pi w_{pl}^2(z)} \tag{5.41}$$

the propagation of higher order modes from a plane 1 to a plane 2 through ABCD-type optics can be calculated by using the ABCD law:

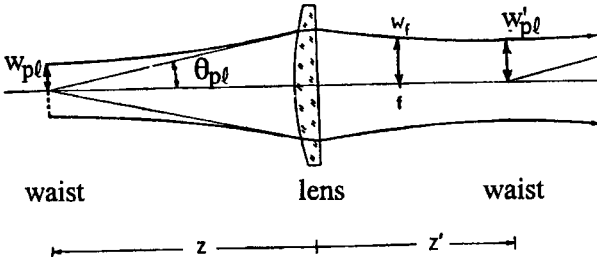


Fig. 5.22 Focusing of transverse modes $TEM_{p\ell}$. The beam waist is imaged at a distance z' from the lens.

$$q_2 = \frac{Aq_1 + B}{Cq_1 + D} \tag{5.42}$$

Note that the q-parameter is the same for all modes including the fundamental mode since the square of the waist is larger by M^2 , which cancels the numerator term in (5.41)! We can use the ABCD law to calculate the focusing properties of the modes. If plane 1 is at the beam waist with radius $w_{p\ell}$ and a focusing lens with focal length f is located at a distance z from the waist, the position z' (measured from the lens) of the focal beam waist with radius $w'_{p\ell}$ are given by (see Fig. 5.22 and Sec. 2.5.1):

$$\frac{1}{z} + \frac{1}{z'} = \frac{1}{f} + \frac{z_0^2}{z[z^2 + z_0^2 - zf]} \tag{5.43}$$

$$w'_{p\ell} = w_{p\ell} \frac{f}{\sqrt{z_0^2 + (z-f)^2}} \tag{5.44}$$

Example (Fig. 5.23):

CO₂ laser, $\lambda=10.6\mu m$, tube diameter $d=30mm$, tube length $l=300mm$, $\rho_1=-5m$, $\rho_2=+5m$, $L=0.5m$. The gas tube is in the middle of the resonator. A focusing lens with $f=100mm$ is located at a distance of $50mm$ from mirror 2. The g-parameters of the mirrors are: $g_1=1.1$ and $g_2=0.9$. With (5.10) and (5.17)-(5.20) we get the following properties of the Gaussian beam:

beam radius at mirror 1	$w_{00}^{(1)}$	= 3.906mm
beam radius at mirror 2	$w_{00}^{(2)}$	= 4.319mm
beam waist	w_0	= 2.897mm
waist position	L_{01}	= -2,250mm
Rayleigh range	z_0	= 2,488 mm
beam radius at left tube end	$w_{00}(z_1)$	= 3.985 mm
beam radius at right tube end	$w_{00}(z_2)$	= 4.233 mm

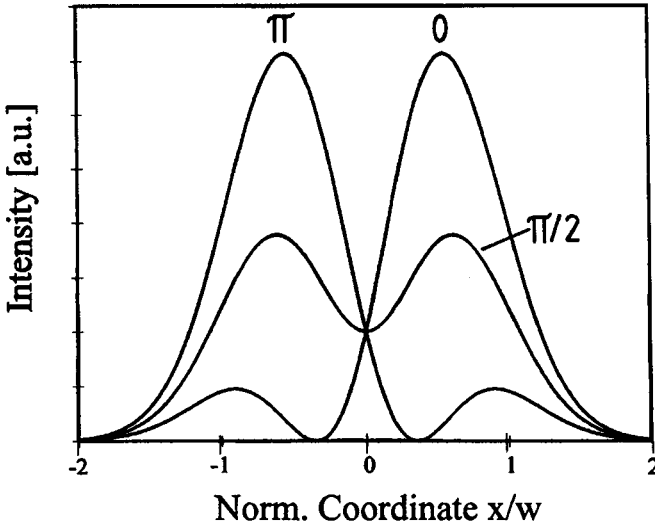


Fig. 5.24 Superposition of a TEM_{00} and a TEM_{10} mode according to (5.41) with $E_0 = E_1$. The different curves depict various phase delays $\phi = \Omega t - \Delta$ between the modes. The curve for $\phi = \pi/2$ represents the time-averaged intensity distribution.

This results in an intensity distribution: (5.46)

$$I(x,z,t) = const. \exp\left[\frac{-2x^2}{w^2}\right] \left(E_0^2 + E_1^2 \frac{8x^2}{w^2} + E_0 E_1 \frac{4\sqrt{2}x}{w} \cos(\Omega t - \Delta) \right)$$

with: $\Omega = 2\pi(v_{q10} - v_{q00}) = \frac{c_0}{L} a \cos\sqrt{g_1 g_2}$ (see Eq. (5.16))

The intensity distribution is the sum of the intensity distributions of the individual modes plus an oscillating term generated by the frequency difference. The oscillation frequency Ω typically is on the order of 100 MHz. Figure 5.24 presents the temporal change of the intensity distribution during one oscillation cycle. If the intensity pattern is recorded, the instrumentation (e.g. CCD camera) will average over the mode oscillations and only the sum of the intensity distributions of the individual modes is observed. However, during short time intervals the intensity can be much higher at certain areas, especially if a high number of modes with varying amplitudes is oscillating. These so-called *hot spots* can induce damage on the surfaces of optical components.

The calculation of the intensity distribution for a high number of modes generally has to be done numerically. For an infinite number of modes, however, the superposition can, in special cases, be performed analytically. In rectangular symmetry, the infinite sum of eigenmodes yields the field distribution:

$$E(x,z,t) = \exp\left[\frac{-x^2}{w^2}\right] \sum_{m=0}^{\infty} E_m H_m\left[\frac{\sqrt{2}x}{w}\right] \exp[i(m+1)(\Omega t - \Delta)] \quad (5.47)$$

If we assume that the field amplitudes are given by $E_m = E_0/m!$, we can use the generating function of Hermite polynomials,

$$\exp[2yt - t^2] = \sum_{m=0}^{\infty} \frac{H_m(y)t^m}{m!},$$

to calculate the intensity distribution. The final expression then reads:

$$I(x,z,t) = \text{const. } E_0^2 \exp\left[-\left(\frac{\sqrt{2}x}{w} - 2\cos(\Omega t - \Delta)\right)^2\right] \quad (5.48)$$

The intensity distribution is Gaussian with a beam radius of $w/\sqrt{2}$ and the whole profile oscillates back and forth in the x-direction with an amplitude of $\sqrt{2}w$, as shown in Fig. 5.25. This effect is referred to as *transverse modelocking*. If we recorded this intensity distribution with a CCD camera we would observe the time-averaged intensity indicated by the dotted line. At any time, however, the peak intensity is more than twice as high!

In contrast to the cases discussed above, the amplitudes E_m of the transverse modes in laser resonators will exhibit temporal variations caused by their interaction in the active medium. Since different modes make use of different gain areas, the gain unused by one mode will allow a different mode to oscillate with an increased amplitude. This mode competition may be such that no steady-state solution for the mode amplitudes is found. Depending on the type of active material and the boundary conditions of the system (e.g. resonator set-up and pumping conditions), this may lead to a periodic, a quasiperiodic, or a chaotic behavior of the laser emission.

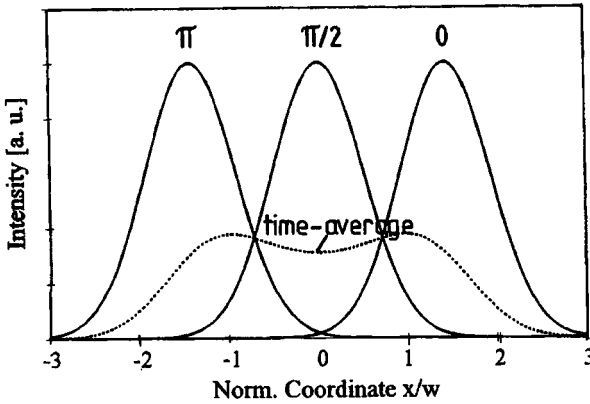


Fig. 5.25 The superposition of an infinite number of Gauss-Hermite modes with Gaussian beam radius w according to Eq. (5.48). The resulting Gaussian intensity profile exhibits temporal oscillations in x -direction with an amplitude of $\sqrt{2}w$. The parameter of the curves is the phase $\phi = \Omega t - \Delta$.

Orthogonality of Transverse Modes

Any field distribution inside or outside of an unconfined stable resonator can be written as a sum of the field distributions of the transverse eigenmodes [3.1, 3.30]. Let us consider Gauss-Hermite eigenmodes in one dimension with field distributions $f_m(x, z)$ at a distance z from the beam waist, given by (5.8). Any field distribution $E(x, z)$ can then be expressed as:

$$E(x, z) = \sum_{m=0}^{\infty} c_m f_m(x, z) \tag{5.49}$$

where c_m is the amplitude (complex number) of each eigenmode. The power of the field distribution is given by:

$$P = \text{const.} \int |E(x, z)|^2 dx = \text{const.} \left[\sum_{m=0}^{\infty} \int |c_m|^2 |f_m(x, z)|^2 dx + \sum_{m=0}^{\infty} \sum_{\substack{n=0 \\ n \neq m}}^{\infty} \int c_m c_n^* f_m(x, z) f_n^*(x, z) dx \right] \tag{5.50}$$

For Gauss-Hermite modes the right-most integral is zero, since:

$$\int_{-\infty}^{\infty} f_m f_n^* dx = \int_{-\infty}^{\infty} H_m \left[\frac{\sqrt{2}x}{x} \right] H_n \left[\frac{\sqrt{2}x}{w} \right] \exp \left[\frac{-2x^2}{w^2} \right] \exp [i(n-m)\Delta] dx = \sqrt{\pi} 2^n n! \exp [i(n-m)\Delta] \delta_{mn} \tag{5.51}$$

with $\delta_{mn} = 1$ for $m = n$ and $\delta_{mn} = 0$ otherwise. The Gauss-Hermite modes thus form an orthogonal set and the total power is the sum of the powers of each mode:

$$P = const. \left[\sum_{m=0}^{\infty} \int |c_m|^2 |f_m(x,z)|^2 dx \right] = \sum_{m=0}^{\infty} P_m \tag{5.52}$$

All modes contain the same power as the fundamental mode, if the amplitudes are given by:

$$c_m = \frac{c_0}{\sqrt{2^m m!}} \tag{5.53}$$

For Gauss-Laguerre modes the orthogonality relation reads: (5.54)

$$\int_0^{2\pi} \int_0^{\infty} f_{pq} f_{q'm}^* r dr d\phi = 2\pi \int_0^{\infty} L_{pq}[t] L_{q'm}[t] t^{l+m} \exp[-t] \exp[i2(q-p)\Delta] r dr = 2\pi \frac{(p+l)!}{p!} \delta_{pq} \delta_{lm}$$

with:
$$t = \left[\frac{2r^2}{w^2} \right]$$

Any field distribution $E(r, \phi)$ can be expressed as a sum of eigenmodes:

$$E(r, \phi, z) = \sum_{p=0}^{\infty} \sum_{l=0}^{\infty} c_{pl} f_{pl}(r, \phi, z) \tag{5.55}$$

Similar to rectangular symmetry, the power is given by the sum of the powers of each mode and the modes exhibit equal power if the following relation holds for the amplitudes:

$$c_{pl} = c_{00} \sqrt{\frac{p!}{(p+l)!}} \tag{5.56}$$

The expansions of a field distribution into the transverse eigenmodes (5.49) and (5.55) are only possible because the Gauss-Hermite and the Gauss-Laguerre modes form a complete set of orthogonal functions. These modes represent the eigenmodes of passive stable resonators with unconfined mirrors. If we insert apertures or an active medium into the resonator, the field distributions of the transverse eigenmodes are changed. The new eigenmodes are generally not orthogonal which means that the total power cannot be expressed as a sum of individual mode powers (the cross integral (5.51) is not equal to zero). We can still expand a field distribution in the resonator as a series of Gauss-Hermite or Gauss-Laguerre modes, but it is mathematically not guaranteed that the power can be expressed as the sum of the powers of the resonator eigenmodes.

5.2.5 Focusability and BeamQuality

The focusing of a laser beam can be considered as the imaging of the beam waist by means of transformation optics such as a lens or a telescope. The position and the beam radius of the focal spot can be calculated by using the Gaussian imaging conditions (5.43) and (5.44). Let w be the beam waist radius of a circularly symmetric beam with Rayleigh range z_0 and θ the corresponding angle of divergence (Fig. 5.26). Two quantities are preserved when the beam is focused no matter what kind of focusing optics are used: the beam parameter product $w\theta$ (we drop the mode indices for simplicity) and the ratio of the cross sectional area in the waist πw^2 to the Rayleigh range z_0 . The following relation holds:

$$\frac{\pi w^2}{z_0} = \pi w\theta \tag{5.57}$$

In order to attain a small focal spot and a large Rayleigh range (remember that this is the distance from the waist at which the beam area has doubled), a low beam parameter product is required. The ratio of the beam area in the focal plane to the Rayleigh range is a characteristic of the laser beam and proportional to the beam parameter product. The ratio cannot be changed by transformation optics. This is shown in Fig. 5.26 in which two different optics are used to focus the same laser beam. It is for this reason that the beam quality is defined via the beam parameter product. The general expression for the beam parameter product, with M^2 being the propagation factor, is given by:

$$w\theta = M^2 \frac{\lambda}{\pi}, \quad M^2 \geq 1 \tag{5.58}$$

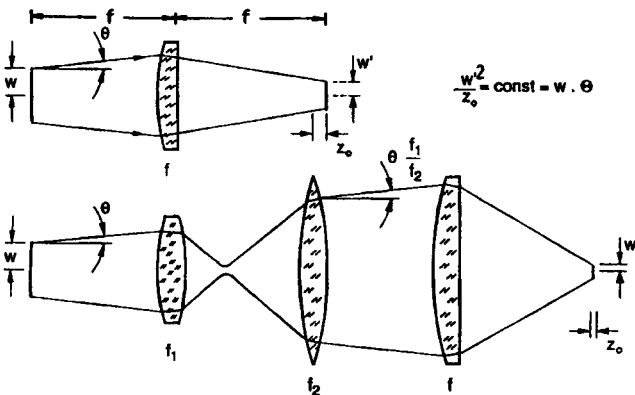


Fig. 5.26 The focusing properties of a laser beam are characterized by the beam waist radius w and the angle of divergence θ . The beam parameter product $w\theta$ determines how small the focal spot area is compared to the Rayleigh range z_0 no matter what type of focusing optics are used.

The propagation factor is equal to 1.0 for the fundamental mode. Both the beam radius and the angle of divergence are defined via the second order intensity moments (see Sec. 2.6). Note that for the same beam, the propagation factor M^2 assumes different values in (5.58) and (5.59) (except for the Gaussian beam where $M^2=1$ in both cases). In order to specify the beam quality it is necessary to measure the beam waist diameter and the angle of divergence separately. This is generally done by generating a waist with a focusing lens and the waist diameter d is determined by the second intensity moment. The corresponding far field with divergence angle can be measured in the focal plane of a second lens (see Chapter 23 for different beam quality measurement techniques). An alternate quantity occasionally used to specify the focusability of a beam is the beam quality factor K defined by:

$$K = \frac{1}{M^2} \quad (5.60)$$

Focusing of Arbitrary Beams to Equal Spot Size

Let us investigate the beam propagation of different quality beams which exhibit the same focal spot radius w_T (Fig. 5.27). For a pure Gaussian beam the following relation holds for the beam radius in the vicinity of the focus:

$$w(z) = w_T \sqrt{1 + \left(\frac{z}{z_0}\right)^2} \quad (5.61)$$

with:
$$z_0 = \frac{\pi w_T^2}{\lambda}$$

For a transverse multimode beam being focused to the same spot size, the corresponding, "embedded", Gaussian beam radius is M times smaller. This results in the propagation law:

$$w(z) = w_T \sqrt{1 + M^2 \left(\frac{z}{z_0}\right)^2} = w_T \sqrt{1 + \left(\frac{z}{z_M}\right)^2} \quad (5.62)$$

with:
$$z_0 = \frac{\pi w_T^2}{\lambda}, \quad z_M = \frac{z_0}{M^2}$$

The Rayleigh range is now shorter by a factor $1/M^2$. This is not in contradiction with (5.35) and Fig. 5.21 where we assumed that higher order modes exhibit an increased beam radius and, therefore, the same Rayleigh range as the Gaussian beam.

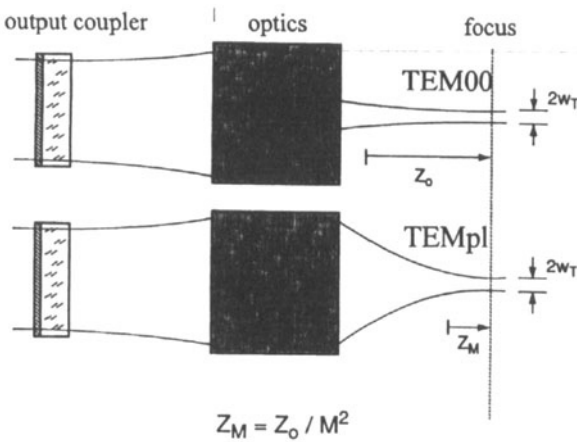


Fig. 5.27 Beam propagation around the focal spot for a fundamental mode and a multimode beam.

Since we now have a fixed beam diameter and more modes have to fit within this diameter, the Rayleigh range will decrease. This behavior is typical for solid-state lasers exhibiting thermal lensing. Attaining a constant focal spot size when the beam propagation factor M^2 changes will be discussed later.

The propagation laws (5.17) and (5.43/5.44) of Gaussian beams can be applied to arbitrary beams if the following transformations are made:

$$\begin{array}{lcl}
 w_0 & \text{-----}> & w_T \\
 z_0 & \text{-----}> & z_M = z_0 / M^2 \\
 \theta_0 & \text{-----}> & \theta
 \end{array}$$

The following relations are useful for the experimental determination of the beam propagation factor:

$$w_T \theta = M^2 \frac{\lambda}{\pi} = \frac{w_T^2}{z_M} \tag{5.63}$$

$$z_M = \frac{\pi w_T^2}{\lambda M^2} \tag{5.64}$$

$$\theta = \frac{w_T}{z_M} \tag{5.65}$$

Note that according to (5.43), the beam propagation factor M^2 also affects the position z' of the image beam waist (Fig. 5.28).

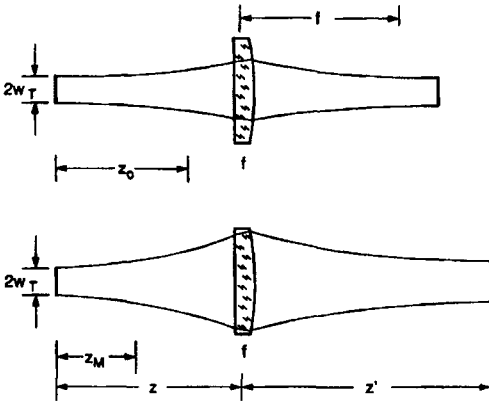


Fig. 5.28 The imaging of a laser beam with beam waist w_T depends on the beam propagation factor M^2 .

Beam Quality and Resonator Parameters

The magnitude of the beam parameter product of a stable laser resonator depends on the number of transverse modes oscillating. The beam propagation factor is determined by the radius and the location of the smallest aperture (with respect to the Gaussian beam radius) inside the resonator. To a very good approximation, the beam propagation factor can be calculated by using (5.38). If b denotes the radius of the active medium with length ℓ and the distances from the endfaces to the nearest mirror are ℓ_1 and ℓ_2 , the beam propagation factor as a function of the resonator parameters reads (Fig. 5.29):

$$M^2 = \frac{\pi b^2}{\lambda L} \frac{|g_1 + g_2 - 2g_1g_2|}{\sqrt{g_1g_2(1 - g_1g_2)}} \left[1 + \frac{[g_1 + g_2 - 2g_1g_2][X - Lg_2(1 - g_1)/(g_1 + g_2 - 2g_1g_2)]^2}{L^2(g_1g_2(1 - g_1g_2))} \right]^{-1} \tag{5.66}$$

with $X = \ell_1 + \ell$ if $L_{01} < \ell_1 + \ell/2$ (see Fig. 5.29 and (5.20))
 $X = \ell_1$ otherwise
 $L = \ell_1 + \ell_2 + \ell$

The same expression holds for rectangular media if the radius b is replaced by half the thickness t of the medium. Once the beam propagation factor M^2 is determined, we can calculate, in addition to the beam parameter product, the beam radius $w(z)$ as a function of the distance z from the waist w , the angle of divergence θ , and the mode volume V inside the resonator by using the corresponding expressions for the fundamental mode (5.17), (5.21), and (5.28):

$$\begin{aligned} w(z) &= w_{00}(z) M \\ \theta &= \theta_0 M \\ V &= V_{00} M^2 \\ w\theta &= w_0\theta_0 M^2 \end{aligned}$$

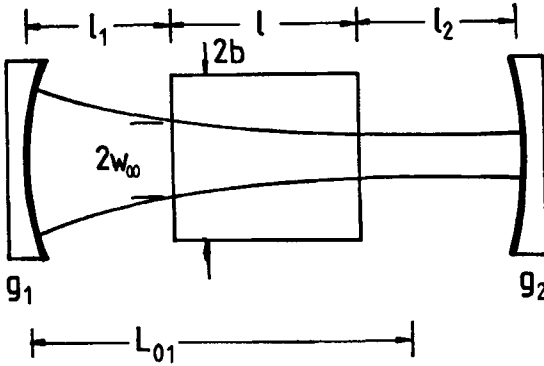


Fig. 5.29 The size of the active medium determines the number of transverse modes. The ratio of the radius b to the largest Gaussian beam radius inside the medium w_{00} determines the beam propagation factor. L_{01} is the distance of the beam waist from mirror 1, given by (5.20).

Figure 5.30 presents the beam parameter product as a function of the g -parameters for stable resonators of equal length $L=1m$ and different locations of the active medium with radius $b=5mm$. The best beam quality is attained near the stability limits at positive g -parameters since the Gaussian beam radii go to infinity in this area. If the active medium is placed in the middle of the resonator, the concentric resonator generally exhibits the worst beam quality. Note that the beam parameter product in multimode operation does not depend on the wavelength! This means that the size of the focal spot does not depend on the type of laser material used. This is due to the fact that a smaller wavelength will generate a smaller radius Gaussian beam which in turn increases the number of transverse modes fitting into the medium. Therefore, the product $M^2 \lambda$ is a constant of the resonator (see (5.66)).

Beam Quality of Laser Systems

We have discussed the beam parameter product and its dependence on the resonator parameters. Now let us generate a small focal spot size for a given laser beam (Fig. 5.31). We focus a beam with a diameter d_0 at the waist and a full angle of divergence Φ , both defined by the second intensity moments (2.93/94) or (2.97/98), by means of a lens with focal length f . According to (5.44), the beam diameter d'_0 in the focus is given by:

$$d'_0 = d_0 \frac{f}{\sqrt{z_M^2 + (z-f)^2}} \tag{5.67}$$

with:
$$z_m = \frac{d_0}{\Phi}$$

and z being the distance of the beam waist d_0 from the lens.

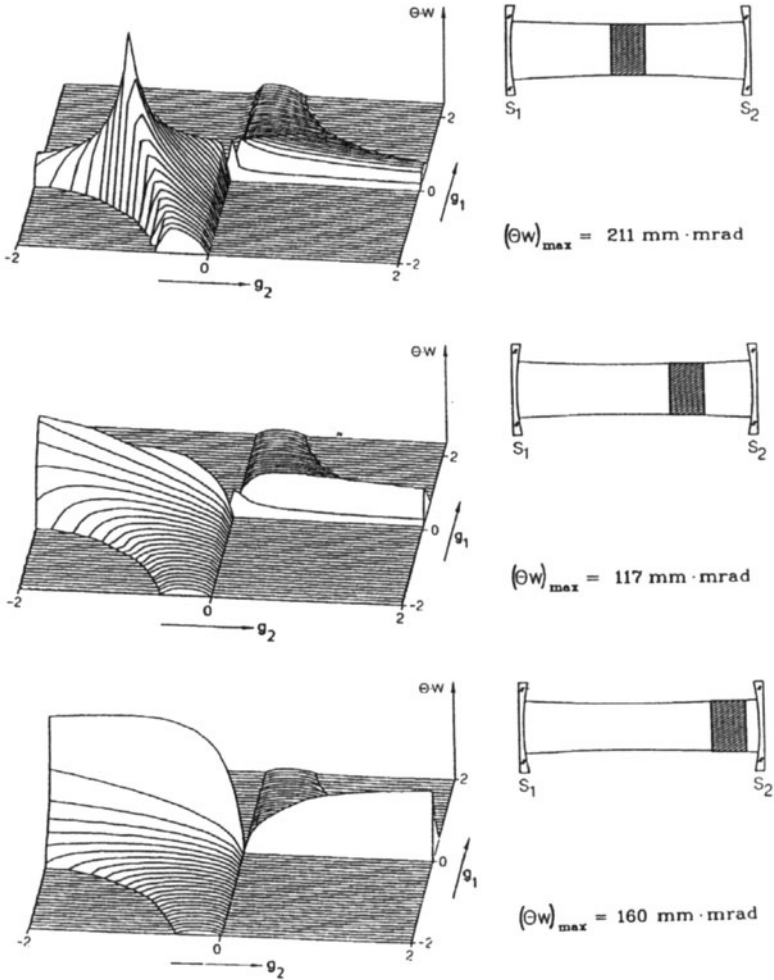


Fig. 5.30 Beam parameter products in the stability diagram for different positions of the active medium ($b=5\text{mm}$, $l=100\text{mm}$). The resonator length is always $L=1\text{m}$. For each graph the maximum beam parameter product is given [S.5].

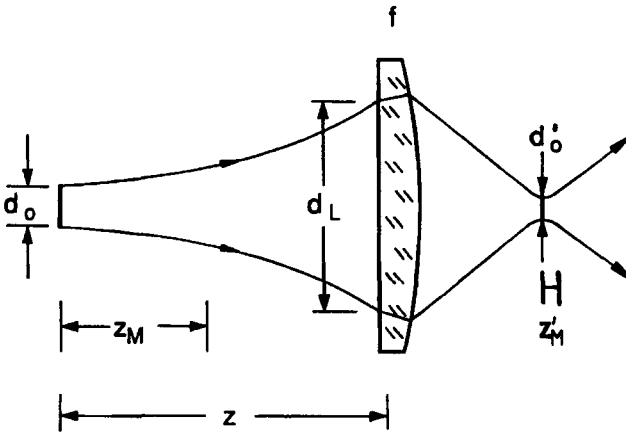


Fig. 5.31 Focusing of a laser beam with beam waist diameter d_0 and angle of divergence $\Phi = d_0/z_M$.

In general, the exact waist position z is not known. This is not a serious problem if we know the beam diameter d_L at the lens. The propagation law (5.62) yields:

$$d_L = \frac{4M^2\lambda}{\pi d_0} \sqrt{z_M^2 + z^2} \quad (5.68)$$

By inserting (5.68) into (5.67) and making the assumption $z \gg f$, we get:

$$d'_0 = \frac{4M^2\lambda f}{\pi d_L} \quad (5.69)$$

The new Rayleigh range z'_M can be calculated with:

$$z'_M = \frac{\pi d_0'^2}{4\lambda M^2} \quad (5.70)$$

Since the beam propagation factor is a constant of the beam, the spot size can be decreased by either using a shorter focal length lens or by increasing the beam diameter at the lens. This is the reason laser beams are generally expanded by means of a telescope in front of the focusing lens. But keep in mind that this will also decrease the Rayleigh range z'_M because the beam parameter product is preserved. Table 5.3 presents typical beam propagation factors M^2 , Rayleigh ranges z'_M , and spot diameters d'_0 for different laser systems. A beam diameter at the focusing lens of $d_L = 10\text{mm}$ (calculated using (5.69) and (5.70)).

Table 5.3 Focusing properties of different laser systems at several output powers (focal length $f=100\text{mm}$, beam diameter at lens $d_L=10\text{mm}$).

Laser	$P_{\text{out}}[\text{W}]$	M^2	$d'_o[\text{mm}]$	$z'_M[\text{mm}]$
HeNe ($\lambda=0.633\mu\text{m}$)	0.005	1	0.008	0.079
Nd:YAG ($\lambda=1.064\mu\text{m}$) (lamp-pumped rod)	20	1	0.0136	0.136
	400	50	0.677	6.77
	1,500	60	0.813	8.13
CO ₂ ($\lambda=10.6\mu\text{m}$)	500	1	0.135	1.35
	3,000	2	0.270	2.70
	10,000	3	0.405	4.05

Special Focusing Optics

1) Focusing of beams with constant beam divergence

For some resonators with an internal variable lens (thermal lensing) the beam waist w is changed as the pump power is increased, whereas the angle of divergence θ remains constant. Despite this behavior a constant spot size can be attained by placing the beam waist in the front focal plane of the focusing lens (Fig. 5.32). In this case the focal spot is found in the back focal plane with $w'=f\theta$.

2) Focusing of beams with constant waist radius

If the beam waist radius stays constant and the angle of divergence varies, focusing optics can also be designed so that the spot size is preserved. This beam behavior is typical for resonators with thermal lensing. Furthermore, the radiation exiting a fiber falls into this category since the core radius of the fiber defines the beam waist. Focusing is accomplished by imaging the beam waist with a telescope with magnification $f_2/f_1 < 1$, as shown in Fig. 5.33. The position z' of the focus and the spot radius w' are given by:

$$z' = -\left(\frac{f_2}{f_1}\right)^2 z + f_2 \left(1 + \frac{f_2}{f_1}\right), \quad w' = w \frac{f_2}{f_1}$$

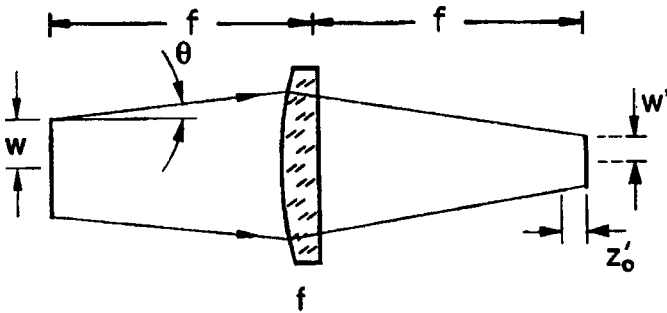


Fig. 5.32 If the beam waist is located at the front focal plane of a focusing lens, the spot radius w' is only a function of the angle of divergence θ and the focal length f .

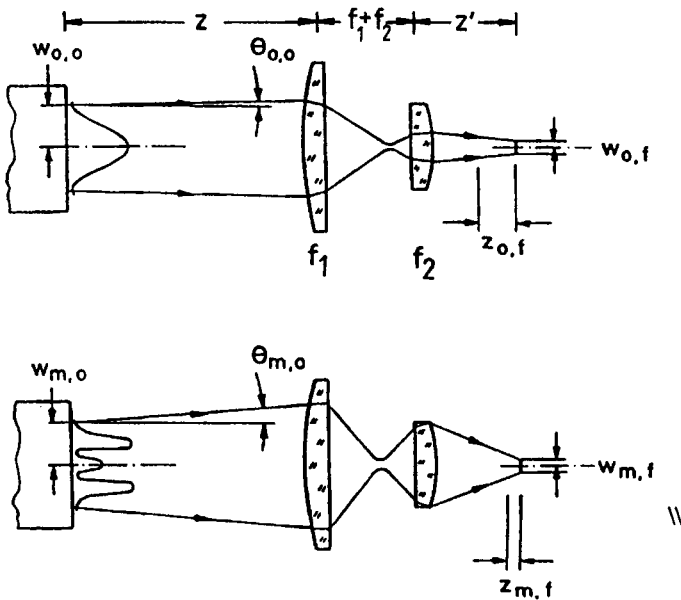


Fig. 5.33 Focusing of laser beams having a constant beam waist by means of a telescope. The higher order mode (lower graph) with its increased angle of divergence exhibits the same spot size as the fundamental mode. The Rayleigh range, however, is decreased.

5.3 Aperture Limited Stable Resonators

In the preceding section we have calculated the transverse eigenmodes for stable resonators without any limiting apertures inside the resonator. We have only used an aperture to determine the maximum number of transverse modes that can oscillate. A transverse mode represented an eigensolution of the resonator if its beam radius was smaller than the aperture radius. However, the aperture will also generate diffraction losses which are the result of a changed transverse mode structure. For instance, if we decrease the aperture radius so that it becomes smaller than the fundamental mode beam radius, the angle of divergence will increase resulting in an increased power fraction hitting the aperture after each round trip (Fig. 5.34). The intensity distribution at the mirrors is no longer Gaussian and the beam propagation inside the resonator does not follow the Gaussian beam propagation rules. The losses of the fundamental mode will decrease as we open the aperture again and the intensity profile will approach that of a Gaussian beam. If the aperture is much larger than the Gaussian beam radius, the diffraction losses go to zero and we will observe the Gaussian beam again. The next higher transverse mode has by then also decreased its diffraction losses far enough to reach the laser threshold. The output beam will then consist of a superposition of the two lowest order transverse modes.

If we plotted the diffraction loss as a function of the aperture radius we would expect a graph as shown in Fig. 5.35 (for circular symmetry). With increasing aperture radius the losses of an increased number of transverse modes will go below a certain loss threshold required to maintain a steady-state oscillation. Since the beam radius is proportional to $\sqrt{2p+l+1}$, it is a reasonable assumption that the diffraction losses of the $TEM_{p,l}$ mode will exhibit the highest slopes if the aperture radius is varied around a value of about $\sqrt{2p+l+1}$ times the Gaussian beam radius.

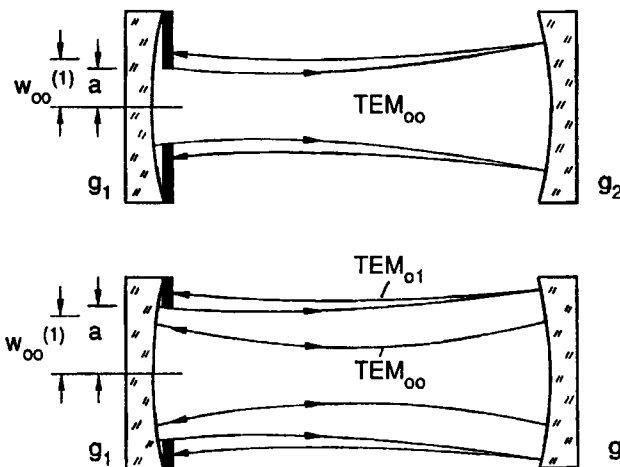


Fig. 5.34 Influence of an aperture on the propagation of the g_2 fundamental mode and the next order transverse mode.

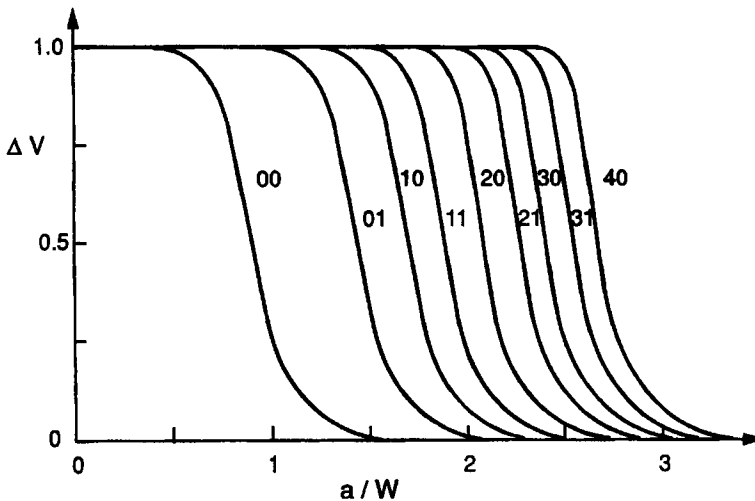


Fig. 5.35 Qualitative dependence of the diffraction losses per round trip of different circularly symmetric modes TEM_{pq} on the ratio of aperture radius to Gaussian beam radius a/w .

The detailed knowledge of the diffraction losses of the transverse modes is crucial for the optimized design of a laser resonator, especially for lasers with low gain media. The pump power required to reach threshold is determined by the losses the radiation experiences in a round trip. The gain factor per transit G_0 has to compensate the losses generated by output coupling and diffraction. The threshold condition reads:

$$G_0 \geq \frac{1}{\sqrt{R_1 R_2} V}$$

where R_i is the reflectance of mirror i , and V is loss factor per round trip ($=1$ -loss). Furthermore, the efficiency of a laser is strongly affected by internal losses. As discussed for the FPI resonator, even low losses in the percent range can decrease the output power by orders of magnitude if the gain of the medium is low. A typical HeNe laser, for instance, would stop laser emission if the losses per round trip were increased only by 1-2%. In this case the resonator design has to be carefully optimized to attain lossless fundamental mode operation while preventing higher order modes from oscillating.

In the following, we will discuss the dependence of the diffraction losses of transverse modes on the g -parameters, the aperture radii, and the number and location of the apertures inserted into the resonator. Our main attention is on the fundamental mode since its losses determine the behavior of the laser at threshold. The time it takes to build up the threshold gain after onset of the pumping, is only affected by the losses of the fundamental mode, even in lasers operating in multiple transverse modes.

5.3.1 One Aperture Limited Mirror

Let us first consider the case that only one aperture is placed inside the resonator directly in front of mirror 1 [3.6,3.7,3.10,3.16-3.20] (Fig. 5.36). The field distributions at mirror 1 are eigensolutions of the Kirchoff integral equation (5.3) for the round trip. However, the integral limits are not infinite, but given by the size of the aperture. In rectangular geometry with an aperture width of $2a$ and an aperture height of $2b$, the integral equation for the fields of the transverse eigenmodes reads:

$$\gamma_{mn} E_{mn}(x_2, y_2) = i \frac{\exp[-ikL]}{2Lg_2\lambda_0} \int_{-b}^b \int_{-a}^a E_{mn}(x_1, y_1) \exp \left[\frac{-i\pi}{2Lg_2\lambda_0} \left(G(x_1^2 + y_1^2 + x_2^2 + y_2^2) - 2(x_1x_2 + y_1y_2) \right) \right] dx_1 dy_1$$

with: $G = 2g_1g_2 - 1$; L : optical resonator length $= nL_0$ (L_0 : geometrical length)
 λ_0 : vacuum wavelength, $k = 2\pi/\lambda_0$: wave number

In circular symmetry with a round aperture with radius a , the corresponding equation is given by:

$$\gamma_{p\ell} E_{p\ell}(r_2, \phi_2) = i \frac{\exp[-ikL]}{2Lg_2\lambda_0} \int_0^{2\pi} \int_0^a E_{p\ell}(r_1, \phi_1) \exp \left[\frac{-i\pi}{2Lg_2\lambda_0} \left(G(r_1^2 + r_2^2) - 2r_1r_2 \cos(\phi_1 - \phi_2) \right) \right] r_1 dr_1 d\phi_1$$

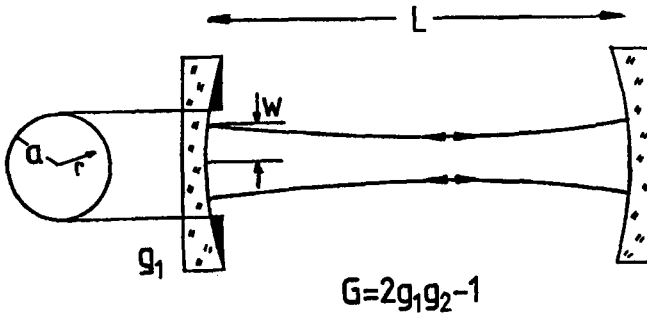


Fig. 5.36 Stable resonator with aperture limited mirror 1 (circular symmetry).

In the following we restrict the discussion to the circularly symmetric resonator. By separating the radial and the azimuthal field components according to:

$$E_{\rho\ell}(r, \Phi) = u_{\rho}(r) \exp[i\ell\Phi]$$

the integration over the azimuthal coordinate can be performed, resulting in:

$$\gamma_{\rho\ell} u_{\rho}(r_2) = (-i)^{\ell} 2\pi N_{eff} \exp[-ikL] \int_0^1 u_{\rho}(r_1) J_{\ell}(2\pi N_{eff} r_1 r_2) \exp[-i\pi N_{eff} G(r_1^2 + r_2^2)] r_1 dr_1$$

with: r_i : normalized radial coordinate (5.73)
 J_{ℓ} : Bessel function of order ℓ
 N_{eff} : effective Fresnel number (see below)

In contrast to the unconfined resonator, the loss factors $V=|\gamma_{\rho\ell}|$ are now lower than 1.0 since the eigenmodes exhibit diffraction losses at the aperture. Eq. (5.68) indicates that the losses and the mode structure depend only on two parameters:

the equivalent G-parameter $G=2g_1g_2-1$
the effective Fresnel number $N_{eff} = a^2/(2Lg_2\lambda_0)$

The effective Fresnel number is proportional to the area of the aperture. Its relationship to the Gaussian beam radius $w_{00}^{(1)}$ at mirror 1 is given by:

$$\left[\frac{a}{w_{00}^{(1)}} \right]^2 = \pi N_{eff} \sqrt{1 - G^2} \tag{5.74}$$

We see that stable resonators in fundamental mode operation with an aperture radius that is 1.2-1.5 times larger than the Gaussian beam radius exhibit an effective Fresnel number around 1.0. All resonators having the same absolute value of the equivalent g-parameter and the same absolute value of the effective Fresnel number exhibit the same eigenmodes and loss factors. These resonators are referred to as equivalent resonators. If we knew the functional relationship between the losses and the resonator parameters $|G|, |N_{eff}|$, we could determine the mode properties of any stable resonator provided that only one mirror is aperture limited.

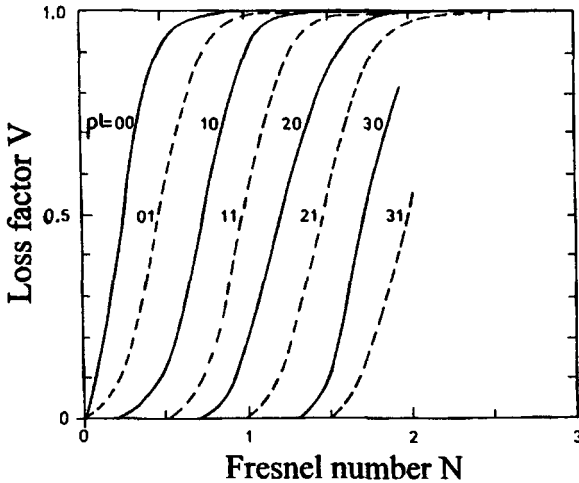


Fig. 5.37 Loss factor per round trip of different transverse modes in circular symmetry for $G=0.0$ as a function of the effective Fresnel number N . The aperture radius is equal to the Gaussian beam radius for $N_{eff}=1/\pi \approx 0.318$.

Examples of equivalent resonators:

- 1) $\rho_1=\infty$, $\rho_2=2\text{m}$, $L=1\text{m}$, $a=0.8\text{mm}$, $\lambda_0=1.064\mu\text{m}$
 -----> $g_1 = 1.0$, $g_2 = 0.5$, $G = 0.0$, $N_{eff} = 0.602$, $a/w_{00}^{(1)} = 1.376$
- 2) $\rho_1=2.5\text{m}$, $\rho_2=1.333\text{m}$, $L=0.5\text{m}$, $a=0.633\text{mm}$, $\lambda_0=1.064\mu\text{m}$
 -----> $g_1 = 0.8$, $g_2 = 0.625$, $G = 0.0$, $N_{eff} = 0.602$, $a/w_{00}^{(1)} = 1.376$
- 3) $\rho_1=0.2777\text{m}$, $\rho_2=0.3077\text{m}$, $L=0.5\text{m}$, $a=0.633\text{mm}$, $\lambda_0=1.064\mu\text{m}$
 -----> $g_1 = -0.8$, $g_2 = -0.625$, $G = 0.0$, $N_{eff} = -0.602$, $a/w_{00}^{(1)} = 1.376$

The integral equation (5.73) generally cannot be solved analytically. Figure 5.37 presents the numerically calculated loss factors of different low order transverse modes as a function of the effective Fresnel number for resonators with $G=0.0$. The curves agree quite well with the expected dependence of Fig. 5.35. Since the losses are now plotted versus the square of the aperture radius, the curves are almost equally spaced.

In order to determine the losses of all transverse modes of a stable resonators, we have to make graphs like the one shown in Fig. 5.37 for all values of the G -parameter between 0.0 and 1.0. This time-consuming procedure is not really necessary since only the properties of the fundamental mode are of practical interest. The loss of the fundamental mode determines both the laser threshold and the efficiency, whereas the losses of higher transverse modes affect only the output power. Figure 5.38 shows calculated loss factors per round trip in fundamental mode operation as a function of the equivalent G -parameter, a comparison with experimental data is shown in Fig. 5.39. As to be expected, the losses are

symmetric at $G=0$ since resonators having the same absolute value of G are equivalent. Note that the diffraction losses for a constant ratio of aperture radius to Gaussian beam radius depend on the G -parameter and go to zero as the G -parameter approaches 1.0. This means that resonators close to the stability limits experience the lowest loss for the fundamental mode. In order to minimize the fundamental mode loss this graph encourages us to increase the aperture radius as much as possible. However, to prevent the next transverse mode from oscillating it is necessary to choose an aperture radius of 1.2-1.4 times the Gaussian beam radius. The larger $|G|$ and the higher the gain of the medium, the closer the aperture radius can approach the Gaussian beam radius.

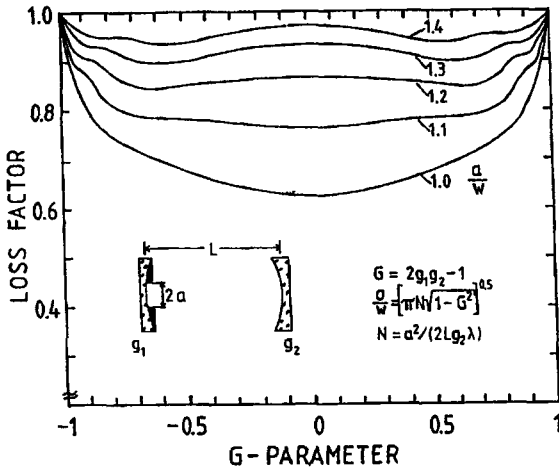


Fig. 5.38 Calculated loss factors per round trip of the fundamental mode in stable resonators with a circular aperture of radius a as a function of the equivalent G -parameter $G=2g_1g_2-1$. The aperture radius is shown normalized to the Gaussian beam radius w .

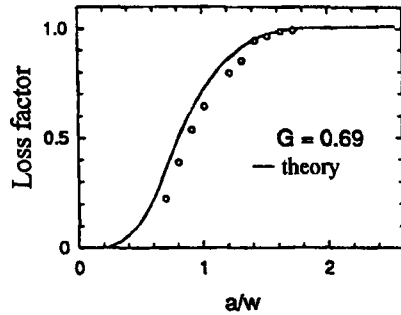
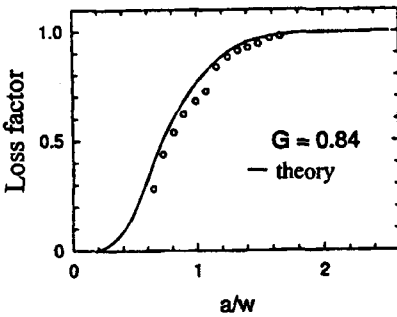


Fig. 5.39 Measured loss factors per round trip as a function of the ratio of the aperture radius a to the Gaussian beam radius w for two different G -parameters. The solid line represents the numerically calculated loss factor [S.6].

The loss per round trip of the fundamental mode and the next transverse mode TEM_{01} can be approximated by using the empirical relation [3.39,3.41]:

$$\Delta V = \exp[-\alpha N_{eff}^{\beta}] \quad (5.75)$$

The parameters α and β read:

G	0.0	0.2	0.4	0.5	0.6	0.7	0.8	0.85	0.9	0.95	0.99
TEM₀₀:											
α	8.4	6.9	4.9	4.4	3.8	3.5	2.9	2.6	2.3	2.0	1.83
β	1.84	1.66	1.38	1.34	1.34	1.27	1.16	1.08	1.01	0.86	0.59
TEM₀₁:											
α	5.1	4.3	2.84	2.46	2.18	1.86	1.5	1.34	1.18	1.05	1.02
β	2.69	2.46	1.91	1.83	1.84	1.81	1.58	1.46	1.35	1.12	0.84

Diffraction Losses in Multimode Operation

If the aperture radius is much larger than the Gaussian beam radius, all transverse modes fitting into the aperture oscillate simultaneously. Only those modes whose beam radii are close to the aperture radius exhibit noticeable diffraction losses. As the aperture is increased the loss of the highest order mode will decrease until the next mode starts oscillating and the loss increases again. The loss will thus show an oscillating behavior as a function of the aperture radius. A numerically calculated example is presented in Fig. 5.40. As soon as the next transverse mode reaches the laser threshold, the loss factor decreases again whereas the mode volume becomes higher due to the larger beam radius of this mode. The oscillation depth will, however, become smaller with increasing aperture radius and the loss factor will slowly approach 1.0. In multimode lasers the number of transverse modes is on the order of 100 resulting in a round trip loss of 1.0-1.5% (Fig. 5.41). This loss has to be taken into account if the output power is calculated (see Chapter 10). Although a loss of 1% seems to be small, it has a considerable effect on the design of high power lasers. For a laser with an output power of 1kW, the intracavity power is typically 2kW which means that a power of 20W falls onto the aperture. Therefore, it is necessary to cool the aperture in order to prevent damage.

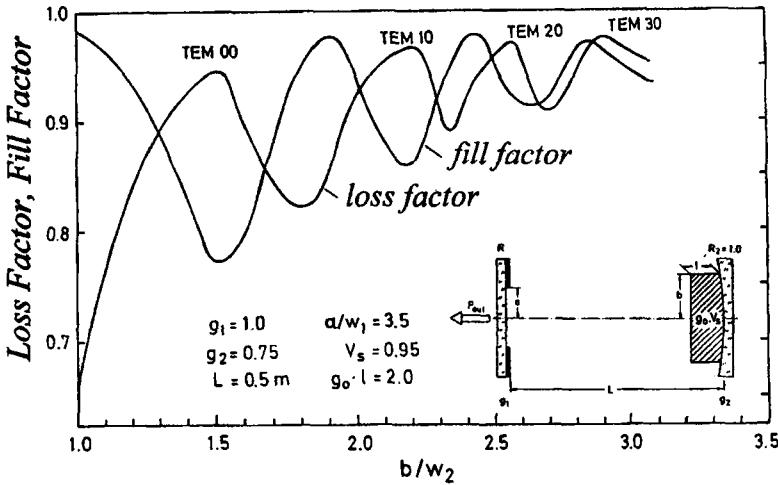


Fig. 5.40 Calculated loss factor per round trip and fill factor (mode volume normalized to the volume of the active medium) for a stable resonator as a function of the ratio of the radius b of the active medium to the Gaussian beam radius w_2 . The aperture radius a at mirror 1 is held constant at $a=3.5w_1$. w_1, w_2 refer to the Gaussian beam radii at mirrors 1 and 2, respectively. The oscillations of both the loss factor and the fill factor become less pronounced as the transverse mode order increases. Only modes without azimuthal structure ($l=0$) were calculated (small signal gain $g_o l = 2.0$, loss factor per transit through the medium $V_s=0.95$).

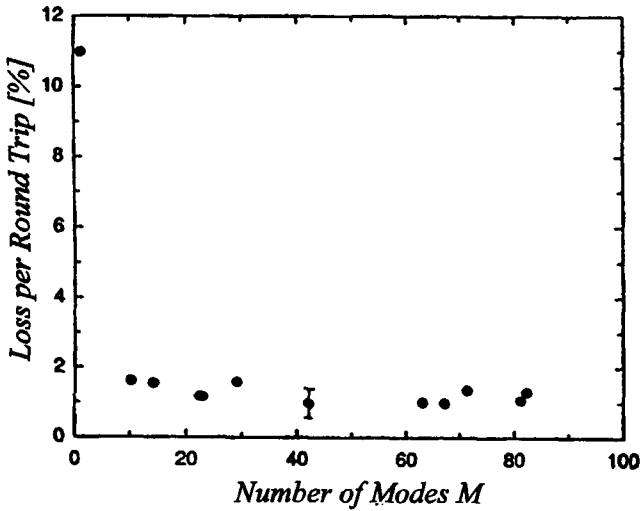


Fig. 5.41 Measured loss per round trip of an Nd:YAG laser in multimode operation as a function of the number of transverse modes M . The loss was determined by measuring the power hitting the aperture with respect to the total intracavity power.

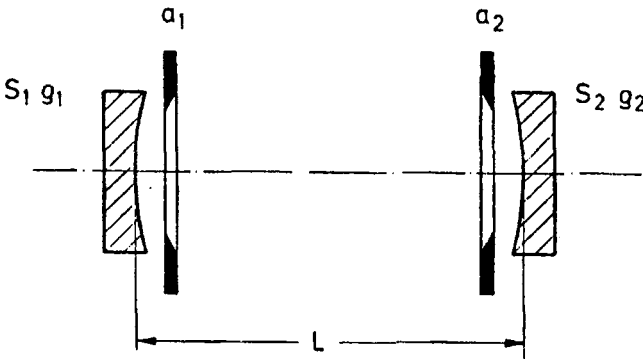


Fig. 5.42 Stable resonator with two aperture limited mirrors.

5.3.2 Both Mirrors Aperture Limited

This case is much more complicated to deal with since the mode properties depend on three parameters rather than only on two parameters. If the aperture radii at mirror 1 and 2 are a_1 and a_2 , respectively (Fig. 5.42), the loss per round trip of each transverse mode is a function of the modified g-parameters $g_1 a_1 / a_2$, $g_2 a_2 / a_1$, and the Fresnel number N with:

$$N = \frac{a_1 a_2}{\lambda L} \tag{5.76}$$

It is, therefore, difficult to present a general overview of the mode properties of these resonators. Furthermore, the number of publications dealing with double aperture resonators is very limited [3.16,3.18,3.35,3.36].

In order to calculate the loss factor and the mode structure we have to apply the Kirchhoff integral to both transits inside the resonator. First we propagate the field from mirror 1 to mirror 2 and then back again. We thus get two coupled integral equations:

$$u_{2p}(r_2) = (-i)^4 2\pi N \exp[-ikL] \int_0^1 u_{1p}(r_1) J_1(2\pi N r_1 r_2) \exp\left[-i\pi N \left(g_1 \frac{a_1}{a_2} r_1^2 + g_2 \frac{a_2}{a_1} r_2^2\right)\right] r_1 dr_1$$

$$\gamma_{p1} u_{1p}(r_1) = (-i)^4 2\pi N \exp[-ikL] \int_0^1 u_{2p}(r_2) J_1(2\pi N r_1 r_2) \exp\left[-i\pi N \left(g_2 \frac{a_2}{a_1} r_2^2 + g_1 \frac{a_1}{a_2} r_1^2\right)\right] r_2 dr_2$$

with

$$\begin{aligned}
 u_{ip}(r_i) &: \text{radial field distribution at mirror } i & (5.77) \\
 r_1, r_2 &: \text{normalized radial coordinates} \\
 N &: \text{Fresnel number} = a_1 a_2 / (\lambda L)
 \end{aligned}$$

The loss per round trip is given by $\Delta V_R = 1 - |\gamma_{pt}|^2$. It is common to define the loss per transit via $\Delta V_T = 1 - \sqrt{|\gamma_{pt}|^2}$, which represents the average loss per transit since the losses are generally different for the two directions. Figure 5.43 presents calculated losses per transit of the TEM₀₀ mode and the TEM₀₁ mode for different resonators as a function of the Fresnel number N for symmetric apertures ($a_1 = a_2 = a$).

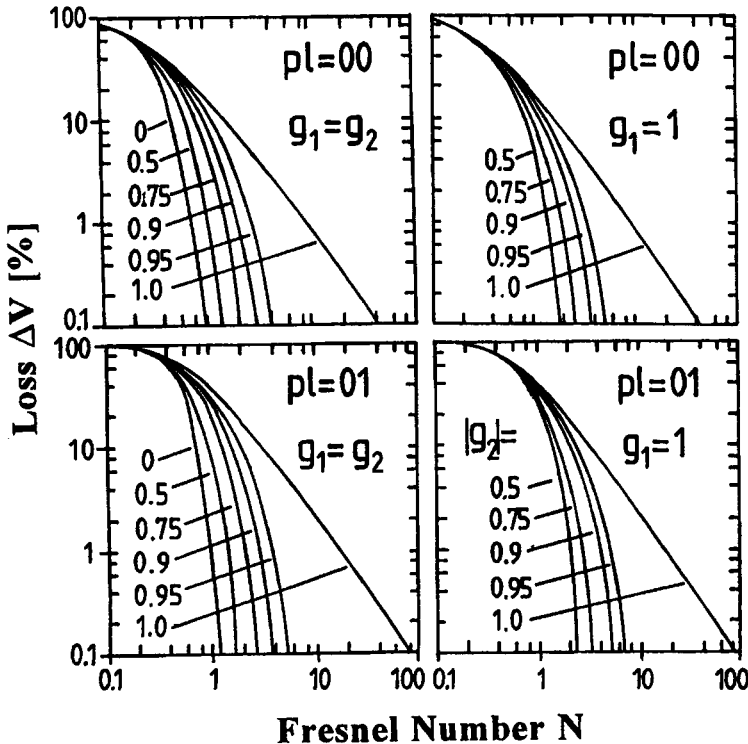


Fig. 5.43 Diffraction losses per transit of stable resonators in circular symmetry with both mirrors limited by apertures with radius $a_1 = a_2 = a$ as a function of the Fresnel number $a^2/(\lambda L)$. The losses for the fundamental mode and the next order transverse mode are shown. The curve parameter is the g -parameter of mirror 2 [after 3.16].

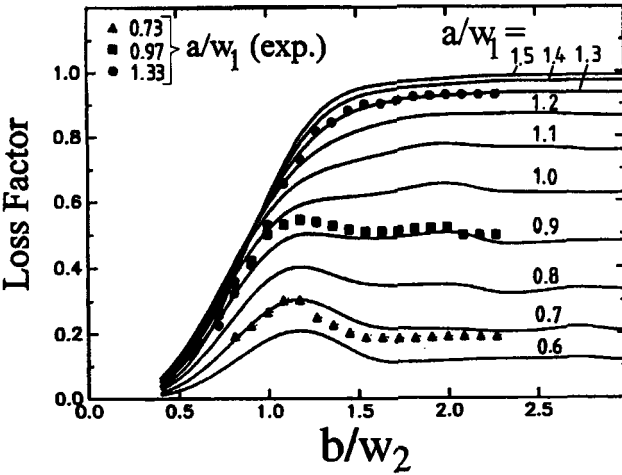


Fig. 5.44 Calculated and measured loss factor per round trip of a stable resonator in fundamental mode operation as a function of the aperture radius b at mirror 2. The curve parameter is the aperture radius a at mirror 1. The Gaussian beam radii at mirror 1 and mirror 2 are w_1 and w_2 , respectively. Note that the losses decrease when the aperture with radius b truncates the Gaussian beam. Resonator parameters: $g_1=1.0, g_2=0.5, L=0.5m$ (pulsed Nd:YAG rod laser, $\lambda=1.064\mu m$).

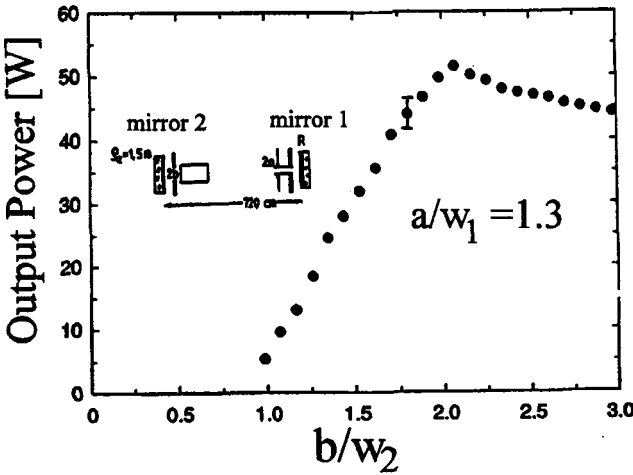


Fig. 5.45 Measured output power per pulse of a stable resonator in fundamental mode operation as a function of the ratio of the aperture radius b to the Gaussian beam radius w_2 at mirror 2. The output coupling mirror 1 is limited by an aperture with radius $a=1.3w_1$. Resonator parameters: $g_1=1.0, g_2=0.56, L=0.66m$ ($6 \times 3/8$ " Nd:YAG rod, small-signal gain $g_0 \ell = 2.2$, reflectance $R=0.7$).

The losses of stable resonator with one aperture limited mirror do not necessarily increase if a second aperture is inserted in front of the second mirror. This is due to the fact that diffraction increases the on-axis intensity. Diffraction at the second aperture, therefore, may decrease the power fraction hitting the first aperture. This effect is shown in Figs. 5.44 and 5.45 for a stable resonator in fundamental mode operation. In both figures, the aperture radius at mirror 1 is remained fixed and the losses and the output power are shown as a function of the radius of the second aperture. If both apertures truncate the Gaussian beam, the loss factor and, consequently, the output power may be higher than with one aperture alone. However, this does not mean that the maximum efficiency in fundamental mode operation is attained with two apertures. In general, the highest output power is achieved if only one aperture is located inside the resonator (see Chapter 11).

The special case of symmetric resonators with both the aperture radius and the radius of curvature being equal for the two mirrors can be discussed by using the properties of an equivalent resonator with one aperture [3.12,3.37]. Any resonator with one aperture limited mirror (mirror 1) and a non-vanishing g -parameter of mirror 2 can be transformed into a symmetric resonator having the same aperture at both mirrors (Fig. 5.46). The transit in this equivalent symmetric resonator is equivalent to the round trip in the resonator with one aperture. The imaging properties of the unconfined mirror 2 are taken into account by changing the resonator length and the mirror curvatures. Since we get the same ray transfer matrix, the loss per round trip in the original resonator with g_1, g_2 and length L is the same as the loss per transit in the equivalent symmetric resonator with g -parameters $G=2g_1g_2-L$ and length $2Lg_2$. The loss per transit of a resonator with $g_1=g_2=g$ and aperture radii $a_1=a_2=a$ can thus be determined by using Fig. 5.38 (and Eq. (5.75) with $G=g$ and $N_{eff}=a^2/(\lambda L)$).

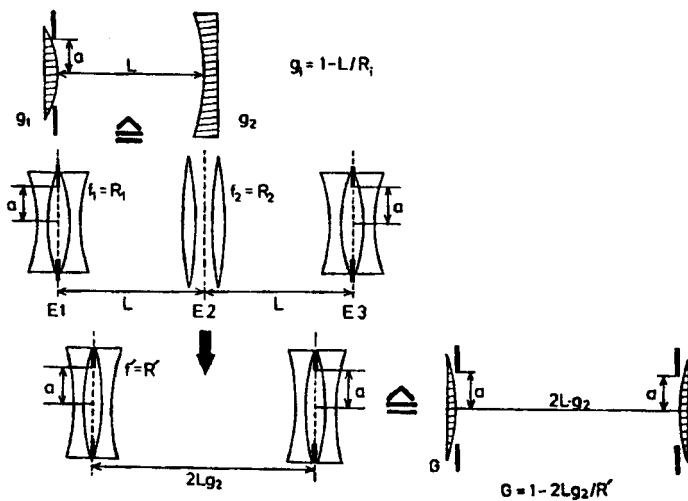


Fig. 5.46 The round trip in a resonator with one aperture is equivalent to a transit in the equivalent symmetric resonator. The transformation between the two resonators is shown with each mirror being replaced by two lenses. The reference planes for the ray transfer matrix are indicated by broken lines. R' denotes the mirror curvature of the equivalent resonator.

5.4 Misalignment Sensitivity

The misalignment sensitivity of a resonator is defined as the sensitivity with which the diffraction losses or the output power are changed due to mirror tilt. In this section we will only discuss the influence of the mirror misalignment on the resonator losses. The resulting variation of the output power will be dealt with in Chapter 14.

The geometrical effect of a mirror tilt is shown in Fig. 5.47 for a resonator with one aperture-limited mirror. Rotation of mirror j by an angle α_j results in a rotation of the optical axis by an angle θ_j with the center of curvature of mirror i being the pivot point. As in the aligned resonator, the optical axis is defined by the line going through the centers of curvature of the mirrors. The angle of rotation of the optical axis θ_j , also referred to as the pointing stability, and the shifts Δ_{ij} , Δ_{ji} of the intersecting points of the optical axis on mirror j and mirror i , respectively, read:

$$\theta_j = \alpha_j \frac{1-g_i}{1-g_1g_2} \tag{5.78}$$

$$\Delta_{ji} = \alpha_j \frac{Lg_i}{1-g_1g_2} \tag{5.79}$$

$$\Delta_{ij} = \alpha_j \frac{L}{1-g_1g_2} \tag{5.80}$$

where g_i is the g -parameter of mirror i , and $i,j=1,2$ with $i \neq j$.

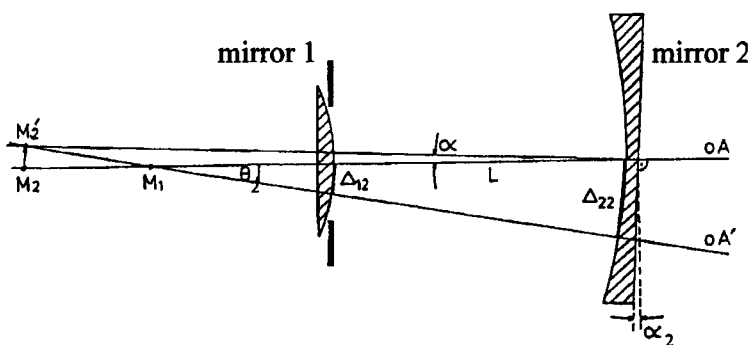


Fig. 5.47 Geometry of mirror misalignment in an optical resonator. Rotation of mirror 2 by α_2 results in a shift of the optical axis by Δ_{12} at mirror 1 and by Δ_{22} at mirror 2. The pointing stability θ and the shifts can be calculated by using (5.78)-(5.80). These equations are also applicable to unstable resonators.

The transverse eigenmodes will keep oscillating parallel to the optical axis whether the resonator is aligned or not. Furthermore, as far as stable resonators are concerned, the mode structure also stays almost symmetric to the optical axis. Since the optical axis comes closer to one side of the aperture if one or both mirrors are tilted, additional diffraction losses are generated. The effective aperture radius is decreased by the shift of the optical axis. In Fig. 5.47 this means that the aperture radius now is $a - \Delta_{12}$ rather than a .

If Δ denotes the total shift of the optical axis at the aperture, to a good approximation, we can describe the properties of the tilted resonator by using an effective Fresnel number $N_{eff}(\alpha)$ which takes the reduction of the aperture into account:

$$N_{eff}(\alpha) = \frac{(a - \Delta)^2}{2Lg_2\lambda_0} \approx N_{eff}(1 - 2\Delta/a) \quad (5.81)$$

The Fresnel number will decrease as the angle of rotation α is increased resulting in an increase of the diffraction losses and a corresponding decrease of the loss factor. For all linear resonators, stable as well as unstable ones, the loss factor decreases parabolically with the angle of rotation for small mirror tilts:

$$V(\alpha) = V(0) \left[1 - 0.1 \left(\frac{\alpha}{\alpha_{10\%}} \right)^2 \right] \quad (5.82)$$

with $V(0)$ being the loss factor for the aligned resonator (Fig. 5.48). The angle $\alpha_{10\%}$ denotes the angle of misalignment at which the loss factor has decreased by 10% and consequently the losses have increased by 10%. This angle is used to define the misalignment sensitivity of optical resonators. A low misalignment sensitivity is equivalent to a small 10%-angle $\alpha_{10\%}$.

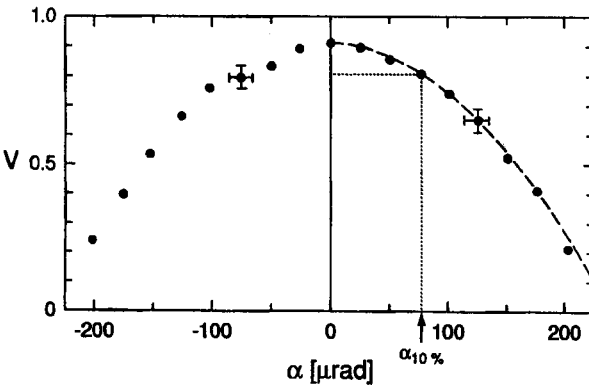


Fig. 5.48 Measured loss factors per round trip of a stable resonator as a function of the angle of misalignment of mirror 2. Mirror 1 is limited by an aperture with radius a ($G=0.34$, $L=0.7\text{m}$, $a=0.55\text{mm}$, $\lambda_0=1.064\mu\text{m}$).

Typical values of $\alpha_{10\%}$ for a stable resonator in fundamental mode operation are on the order of $50 \mu\text{rad}$. The exact value of the 10%-angle depends on the g-parameters of the mirrors, the Fresnel number, the resonator length, and the aperture radii. All resonators exhibit two 10%-angles, each corresponding to the tilt of one mirror. It is customary to define an average misalignment sensitivity by taking the geometrical mean value of the two 10%-angles:

$$\alpha_{10\%} = \frac{1}{2} \sqrt{\alpha_{10\%,1}^2 + \alpha_{10\%,2}^2} \tag{5.83}$$

with the additional indices indicating the corresponding mirror. This mean angle defines the average angle by which both mirrors can be rotated simultaneously before a 10% increase in diffraction losses is generated.

A theoretical investigation of the Kirchhoff integral for misaligned resonators shows that the 10%-angle is proportional to the resonator length and inversely proportional to the aperture radius. In order to compare the misalignment sensitivity of different resonators it is, therefore, advantageous to introduce the misalignment parameter D_i for the mirrors:

$$D_i = \frac{L}{a} \alpha_{10\%,i} \quad , \quad i=1,2 \tag{5.84}$$

The misalignment parameters of the two mirrors depend only on the g-parameters and on the effective Fresnel number.

5.4.1 One Aperture Limited Mirror

Let us consider a resonator with mirror 1 being limited by an aperture with radius a and with the unconfined mirror 2 being misaligned by an angle α_2 , as shown in Fig. 5.47. The mode structures and the diffraction loss can be calculated as a function of the angle of misalignment by using a two-dimensional Kirchhoff integral. Starting at mirror 1 with the field $E(r, \phi)$, the round trip in the resonator reads:

$$\gamma E(r_2, \phi_2) = -i \exp[ikL] N_{eff} \exp\left[\frac{-8\pi i D_2^2}{G-1}\right] \cdot \tag{5.85}$$

$$\cdot \int_0^{2\pi} \int_0^1 E(r_1, \phi_1) K(r_1, r_2, \phi_1, \phi_2) \exp[i4\pi D_2 N_{eff} (r_1 \cos\phi_1 + r_2 \cos\phi_2)] r_1 dr_1 d\phi_1$$

where K is the kernel of the aligned resonator according to (5.67) and r_i being the normalized radial coordinates.

The resonator properties depend on the equivalent G-parameter $G=2g_1g_2-1$, the effective Fresnel number N_{eff} and the misalignment parameter D_2 . Figure 5.49 presents the calculated misalignment parameter D_2 for stable resonators in fundamental mode operation as a function of the effective Fresnel number N_{eff} for different equivalent G-parameters G . The comparison with experimental data is shown in Fig. 5.50.

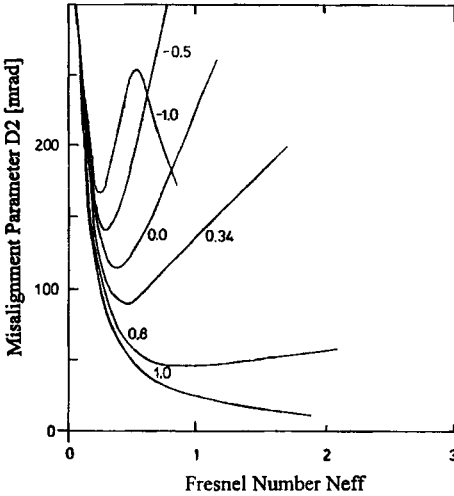


Fig. 5.49 Calculated misalignment parameter for stable resonators in fundamental mode operation as a function of the effective Fresnel number $N_{eff}=a^2/(2Lg_2\lambda_0)$. Mirror 1 is limited by the aperture and the unconfined mirror is tilted (circular symmetry).

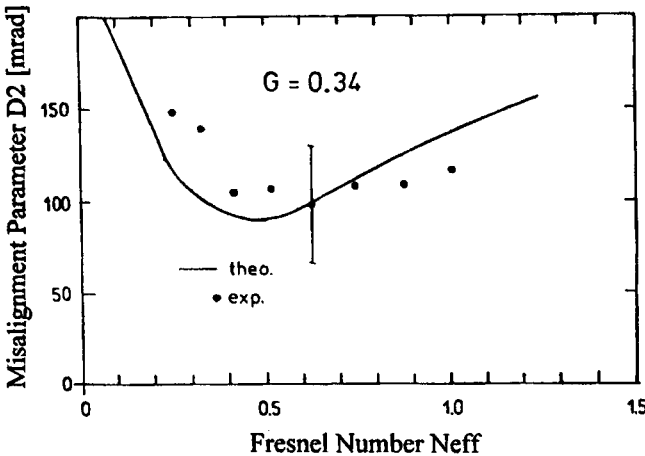


Fig. 5.50 Calculated and measured misalignment parameter D_2 for resonators in fundamental mode operation with $G=0.34$ as a function of the effective Fresnel number. Mirror 1 is aperture limited and the unconfined mirror 2 is misaligned (circular symmetry, Nd:YAG laser, $\lambda_0=1.064\mu\text{m}$).

Of particular interest are resonators in fundamental mode operation with the aperture a being adapted to the Gaussian beam radius w_{00} . Figure 5.51 shows the misalignment parameter of the unconfined mirror for stable resonators with $a/w_{00}=1.3$. This figure indicates how strongly the misalignment sensitivity depends on the location of the resonator in the stability diagram. Note that the misalignment parameter is not a function of the wavelength λ_0 because the ratio of aperture radius to Gaussian beam radius is only a function of N_{eff} and G (see (5.74)). However, the Gaussian beam radius, and therefore the aperture radius a , are proportional to $\sqrt{\lambda_0 L}$ (see (5.10)) which means that the 10%-angle is larger for longer wavelength lasers. The lowest misalignment sensitivity is attained near the axes of the stability diagram ($G=-1$), whereas concave-convex resonators with G being close to $+1.0$ exhibit a sensitivity to mirror tilt. A high mode volume of the fundamental mode (see Fig. 5.19) and a low misalignment sensitivity, therefore, can generally not be achieved simultaneously.

So far we have discussed only the misalignment of the unconfined mirror 2 which results in a shift Δ_{12} at the aperture limited mirror 1. If mirror 1 is tilted we get a shift Δ_{11} at mirror 1. If both mirrors are rotated by the same angle the two shifts are related to each other via:

$$\Delta_{11} = \Delta_{12} g_2 \tag{5.86}$$

A rotation of the unconfined mirror 2 by an angle α is thus equivalent to the rotation of the aperture limited mirror 1 by the angle α/g_2 . The misalignment parameter D_1 can be calculated by dividing the misalignment parameter D_2 by the g -parameter of mirror 2. We can now determine the sensitivity of all resonators in fundamental mode operation to tilt of one of the two mirrors by using Figs. 5.49-5.51.

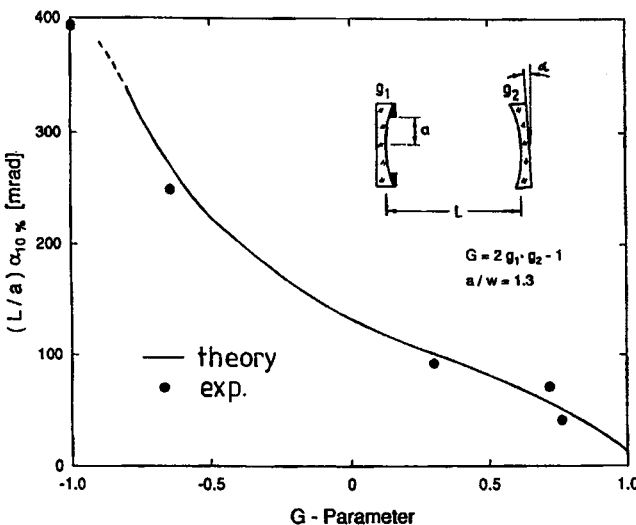


Fig. 5.51 Measured and calculated misalignment parameter D_2 of stable resonators in fundamental mode operation with the aperture radius a at mirror 1 being adapted to the Gaussian beam radius ($a/w_{00}=1.3$). The unconfined mirror 2 is misaligned.

The mean 10%-angle is given by:

$$\alpha_{10\%} = \frac{a}{2L} \sqrt{D_2^2 + D_1^2} = \frac{a}{2L} D_2 \sqrt{1 + (1/g_2)^2} \tag{5.87}$$

For reliable operation as well as safe shipping and handling of the laser system, each mirror should not be misaligned by more than this mean angle. This defines the tolerances required for the stability of the mirror mounts. Resonators with $g_2=0$ exhibit the lowest misalignment sensitivity. Misalignment of mirror 1 does not increase the losses at all (in the geometrical model used we do not get a shift of the optical axis intersection point on mirror 1 since the center of curvature of mirror 2 is located at this mirror) and the sensitivity of mirror 2 to tilt is low compared to other stable resonators (see Fig. 5.51).

Example: Misalignment Sensitivity of a CO₂ Laser Resonator

Resonator geometry: $\rho_1=3m, \rho_2=-4m, L=1m, \lambda_0=10.6\mu m, g_1=0.667, g_2=1.25$. The cylindrical gas tube with diameter $2a=8.75mm$ is positioned close to mirror 1. The Gaussian beam radius at mirror 1 is 3.37mm which means that the ratio of the tube radius to the Gaussian beam radius is 1.3. With $G=2g_1g_2l=0.666$, Fig. 5.51 yields a misalignment parameter of about $D_2=75mrad$. The 10%-angles for the misalignment of the mirrors are:

$$\alpha_{10\%,2} = \frac{a}{L} D_2 = 0.328 \text{ mrad} , \quad \alpha_{10\%,1} = \frac{\alpha_{10\%,2}}{g_2} = 0.263 \text{ mrad}$$

These values result in a mean 10%-angle of 0.21 mrad.

Multimode Operation

If the aperture radius is much larger than the Gaussian beam radius, higher order modes will also oscillate in the misaligned resonator. The diffraction losses, however, will only increase if the optical axis is rotated so far that the Gaussian beam gets limited by the aperture. For smaller tilts, the misalignment only results in a decrease in the number of transverse modes without noticeably increasing the diffraction losses (Fig. 5.52). However, the output power will show a decrease since the mode volume becomes smaller as the mirrors are tilted.

If $K=1/M^2$ denotes the beam quality factor of the aligned resonator (see (5.60) and (5.66)), the 10%-angle in multimode operation, to a good approximation, is given by:

$$\alpha_{10\%,pt} = \frac{1}{\sqrt{K}} \alpha_{10\%,00} \tag{5.88}$$

with $\alpha_{10\%,00}$ being the 10%-angle for fundamental mode operation with adapted aperture radius $a/w_{00}=1.3$.

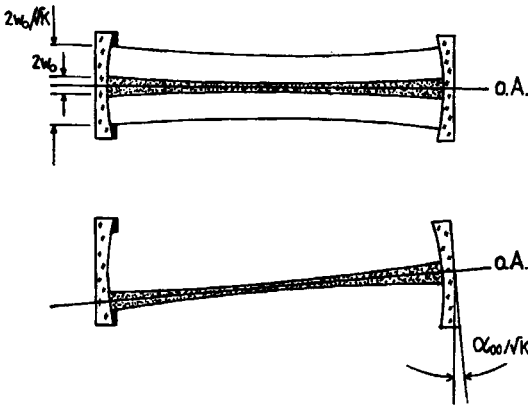


Fig. 5.52 Mirror misalignment in a multimode stable resonator results in an increase in diffraction losses as soon as the fundamental mode gets clipped by the aperture. Since the Gaussian beam radius is \sqrt{K} times smaller than the multimode beam radius (K : beam quality factor, $K < 1$), the multimode 10%-angle is $1/\sqrt{K}$ times larger than the 10%-angle for fundamental mode operation.

5.4.2 Two Aperture Limited Mirrors

If both mirrors are limited by apertures, the mirror misalignment generates additional diffraction losses at both apertures (Fig. 5.53). Similar to the aligned resonators, the theoretical investigation is more complicated and beyond the scope of this book. In the following we will summarize the main results for fundamental mode operation [3.27,3.33]. Let both aperture radii a_1, a_2 be adapted to the Gaussian beam radii $w_{00}^{(1)}, w_{00}^{(2)}$ at the mirrors:

$$a_i = s w_{00}^{(i)} \tag{5.89}$$

If mirror i is misaligned by an angle α_i , a first order perturbation analysis of the diffraction integral yields for the loss factor per round trip [3.33]:

$$V(\alpha_i) = V(0) \left[1 - \alpha_i^2 \frac{s^2}{\exp[2s^2] - 1} D_i^2 \right] \tag{5.90}$$

with:
$$D_i^2 = \frac{\pi L^*}{\lambda_0} \sqrt{\left(\frac{g_j}{g_i} \right)} \frac{1 + g_1 g_2}{(1 - g_1 g_2)^{1.5}}$$

- $L^* = L_0(n-1)/n$: effective resonator length
- L_0 : geometrical resonator length
- n : index of refraction of active medium
- ℓ : length of active medium.

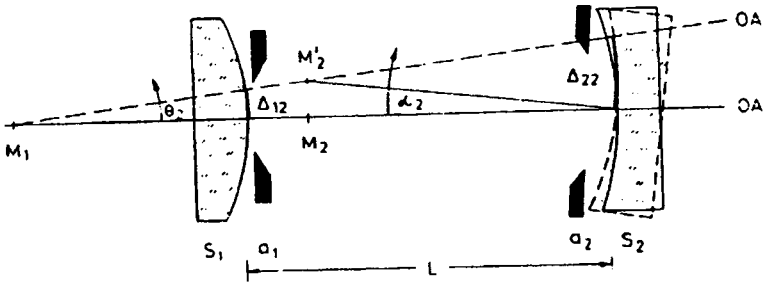


Fig. 5.53 Misalignment of a resonator with both mirrors aperture limited [3.33] (© OSA 1980).

The 10%-angle for the misalignment of mirror i thus reads:

$$\alpha_{10\%,i} = \sqrt{0.1} \frac{\sqrt{\exp[2s^2]-1}}{sD_i} \quad (5.91)$$

If both mirrors are misaligned, the 10%-angle is given by:

$$\alpha_{10\%} = \sqrt{0.1} \frac{\sqrt{\exp[2s^2]-1}}{s\sqrt{D_1^2+D_2^2}} = \sqrt{0.1} \frac{\sqrt{\exp[2s^2]-1}}{sD} \quad (5.92)$$

with:

$$D = \sqrt{\left(\frac{\pi L}{\lambda_0}\right) \frac{1+g_1g_2}{(1-g_1g_2)^{1.5}} \frac{|g_1+g_2|}{\sqrt{g_1g_2}}}$$

We define D as the misalignment sensitivity of the resonator since a small value of D results in a large 10%-angle. Figure 5.54 presents calculated misalignment sensitivities D of stable resonators in fundamental mode operation with both apertures adapted to the Gaussian beam radii at the corresponding mirror. The misalignment sensitivity in this graph is normalized to the sensitivity D_0 of the symmetric confocal resonator with $g_1=g_2=0$, given by:

$$D_0 = \sqrt{\frac{2\pi L}{\lambda_0}} \quad (5.93)$$

The misalignment sensitivity is only a function of the resonator length and the g -parameters.

Lowest misalignment sensitivities again are attained for resonators near the axes of the stability diagram. Figure 5.55 shows a comparison of measured 10%-angles with the theoretical prediction given by (5.91).

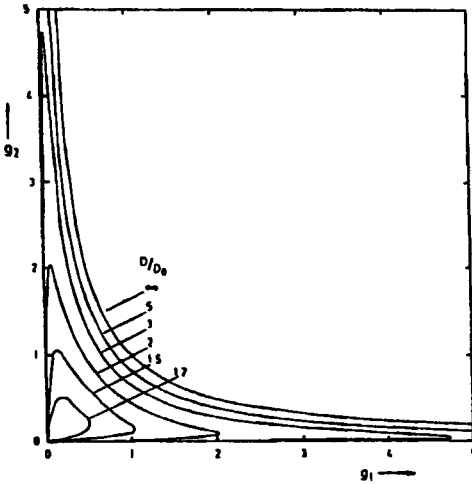


Fig. 5.54 Curves of constant misalignment sensitivity D for resonators with both apertures adapted to the Gaussian beam radius. D_0 is the sensitivity of the confocal resonator [3.33] (© OSA 1980).

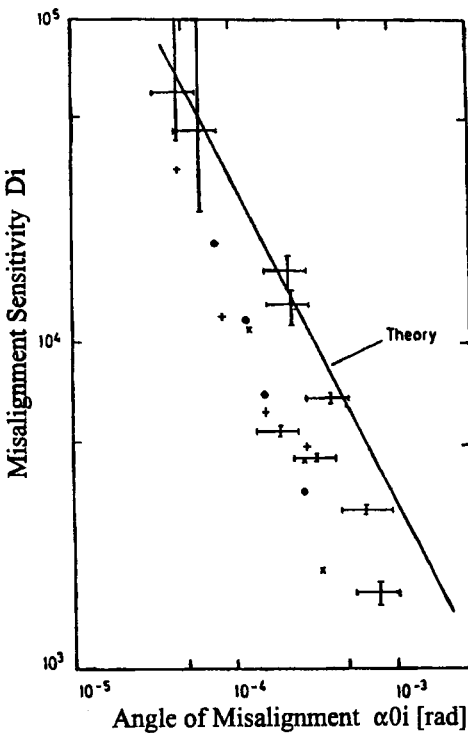


Fig. 5.55 Measured angles of misalignment $\alpha_{0i} = \alpha_{10\%} / \sqrt{0.1}$ and the corresponding misalignment sensitivities D_i of the resonators according to (5.90). The solid line represents relation (5.91) [3.33] (© OSA 1980).